RM H55E31a

NACA

RESEARCH MEMORANDUM

EFFECT OF SEVERAL WING MODIFICATIONS ON THE LOW-SPEED STALLING CHARACTERISTICS OF THE DOUGLAS D-558-II RESEARCH AIRPLANE

By Jack Fischel and Donald Reisert

High-Speed Flight Station
Edwards, Calif.

NATIONAL ADVISORY COMMITTEE
FOR AERONAUTICS

WASHINGTON

July 18, 1955

NATIONAL ADVISORY COMMITTEE FOR AERONAUTICS

RESEARCH MEMORANDUM

EFFECT OF SEVERAL WING MODIFICATIONS ON THE LOW-SPEED STALLING CHARACTERISTICS OF THE DOUGLAS D-558-II RESEARCH AIRPLANE

By Jack Fischel and Donald Reisert

SUMMARY

The low-speed stalling and lift characteristics of the Douglas D-558-II airplane were measured in a series of 1 g stall approaches performed with several wing modifications designed to alleviate swept-wing instability and pitch-up. The airplane configurations investigated include the basic wing configuration and two wing-fence configurations in combination with retracted, free-floating, or extended slats, and a wing leading-edge chord-extension configuration. All configurations were investigated with flaps and landing gear retracted and extended at an altitude of about 20,000 feet.

With slats, flaps, and landing gear retracted, none of the wing modifications investigated had an appreciable effect on the lift or stability characteristics at low and moderate angles of attack. Regardless of wing-fence configuration, appreciably larger values of peak normal-force coefficient were attained with slats unlocked (free floating) or fully extended than with slats closed. Wing fences and the chord-extension tended to delay the onset of instability with slats retracted, and the stable region was further extended for the configurations with either no wing fences or inboard wing fences when the slats were free floating or extended.

With flaps and landing gear extended, only the fully extended slat configuration affected the variation of normal-force coefficient with angle of attack by increasing this variation slightly. Peak values of normal-force coefficient attained were the same for all configurations except the chord-extension configuration. For this configuration excessive buffeting caused earlier termination of the maneuver. Most of the configurations had little or no effect on the stability characteristics over most of the lower and moderate angle-of-attack range. The airplane appeared somewhat more stable, however, with no wing fences installed than with wing fences installed when the slats were extended. At larger angles of attack and with slats extended, inboard wing fences materially improved the stability characteristics of the airplane.

At any given angle of attack, wing flaps provided an increment in normal-force coefficient of about 0.3; whereas, the free-floating or fully extended slats provided zero incremental lift except at very large angles of attack. The airplane generally appeared more stable longitudinally at comparable speeds with flaps deflected than with flaps retracted, but marginal dynamic lateral stability was evident for several configurations with flaps extended or retracted.

In general, adequate stall warning in the form of buffeting was noted by the pilot in the stable region of flight, particularly for the chord-extension configuration for which buffeting appeared aggravated.

INTRODUCTION

As a part of the cooperative Air Force—Navy—NACA high-speed flight program, the National Advisory Committee for Aeronautics is conducting a flight-research program utilizing the Douglas D-558-II swept-wing research airplane. During the course of this flight program, the effects of various modifications designed to alleviate swept-wing instability and pitch-up were investigated from stalling speed up to a maximum Mach number of about 1.0 (refs. 1 to 3). The airplane configurations investigated include the basic wing configuration and two wing-fence configurations in combination with retracted, free-floating, or extended slats, and a wing leading-edge chord-extension configuration. The results of the low-speed stalling characteristics of the airplane in each of the aforementioned configurations, with flaps and landing gear retracted and extended, are presented in this paper.

SYMBOLS

b	wing span, ft
C_{N_A}	airplane normal-force coefficient, nW/qS
c	wing chord, ft
$\bar{c}$	wing mean aerodynamic chord (M.A.C.), ft
F_a	aileron control force, lb
F_e	elevator control force, lb
F_r	rudder control force, lb

g	acceleration due to gravity, ft/sec^2
h_p	pressure altitude, ft
i_t	stabilizer setting with respect to fuselage center line, positive when leading edge of stabilizer is up, deg
M	free-stream Mach number
n	normal load factor or acceleration, g units
q	free-stream dynamic pressure, lb/sq ft
S	wing area, sq ft
t	time, sec
V_i	indicated airspeed, mph
W	airplane weight, lb
α	angle of attack of airplane center line, deg
β	angle of sideslip, deg
δ_a	total aileron position, deg
δ_e	elevator position with respect to stabilizer, deg
δ_r	rudder position with respect to vertical tail, deg
δ_s	slat position, in.
$\dot{\theta}$	pitching velocity, radians/sec
$\dot{\varphi}$	rolling velocity, radians/sec
$\dot{\psi}$	yawing velocity, radians/sec

AIRPLANE

The Douglas D-558-II airplane used in this investigation is equipped with both a Westinghouse J34-WE-40 turbojet engine, which exhausts out the bottom of the fuselage between the wing and the tail, and a Reaction

Motors, Inc. LR8-RM-6 rocket engine, which exhausts out the rear of the fuselage. The airplane is air-launched from a Boeing B-29 mother airplane. A photograph of the airplane is shown in figure 1 and a three-view drawing is shown in figure 2. Pertinent dimensions and characteristics of the unmodified airplane are listed in table I.

For the present series of tests several wing-fence configurations were investigated in combination with several slat configurations. A wing leading-edge chord-extension was also investigated. The fence configurations are shown in figures 3 and 4. The inboard wing fences were incorporated in the original airplane configuration to improve the longitudinal stability characteristics of the airplane at low speeds and at high angles of attack ($\alpha > 10^{\circ}$) when the wing slats were fully extended (ref. 4). The outboard wing fences were similar to the optimum fence configuration developed in the wind-tunnel investigation of reference 4 for improving the longitudinal stability characteristics at high angles of attack in the airplane clean condition. The wing slats (figs. 5 and 6) may be locked in either the open (extended) or closed (retracted) position, or they may be unlocked (free floating). In the unlocked condition they are normally closed at low values of angle of attack or normal-force coefficient and open with increase in angle of attack. The left and right wing slats are interconnected and always have approximately the same position.

The wing leading-edge chord-extensions shown in figures 7 and 8 were similar to those tested in the wind tunnel and found to provide an improvement in static longitudinal stability at moderate angles of attack (refs. 5, 6, and unpublished data). These chord-extensions were approximately the NACA 63-008 airfoil profile in the streamwise direction and were faired into the wing profile over the span of the chord-extensions. In addition, the chord-extensions were faired into the wing tips and the inboard ends were flat-sided in the vertical streamwise plane. For this configuration the wing slats were locked closed and all fences were removed. Addition of the wing chord-extensions increased the wing area from 175 square feet to 181.2 square feet and the wing mean aerodynamic chord from 87.3 inches to 90.0 inches. For convenience in comparison of the data with data for the unmodified airplane, however, all data presented are based on the dimensions of the unmodified airplane.

The airplane is equipped with an adjustable stabilizer but there are no means provided for trimming out aileron- or rudder-control forces. No aerodynamic balance or control-force boost system is used on any of the controls. Hydraulic dampers are installed on all control surfaces to aid in the prevention of control-surface "buzz." Dive brakes are located on the rear portion of the fuselage.

Figure 9 shows the friction in the elevator-control system as measured on the ground under no load as the control was deflected slowly.

The rate of control deflection was sufficiently low so that the control force resulting from the hydraulic damper in the control system was negligible.

INSTRUMENTATION

Among the standard NACA recording instruments installed in the airplane to obtain flight data were instruments which measured the following quantities pertinent to this investigation:

- Airspeed
- Altitude
- Angle of attack
- Angle of sideslip
- Normal acceleration
- Rolling, yawing, and pitching velocities
- Stabilizer, elevator, aileron, rudder, and slat positions
- Aileron and elevator wheel force
- Rudder pedal force

All instruments were synchronized by means of a common timer.

The elevator and rudder positions were measured at the inboard end of each control surface; the left and right aileron positions were measured on bell cranks about 1 foot forward of the ailerons; and the stabilizer position was measured at the plane of symmetry. All control positions were measured perpendicular to the control hinge line.

An NACA high-speed pitot-static tube (type A-6 of ref. 7) was mounted on a boom $4\frac{3}{4}$ feet forward of the nose of the airplane. The vanes used to measure the angle of attack and angle of sideslip were mounted on the same boom about $3\frac{1}{2}$ feet and 3 feet, respectively, forward of the nose of the airplane. Angle of attack and angle of sideslip are presented as measured with only instrument corrections applied. However, any inherent errors, such as caused by upwash effects, are believed to have a negligible effect on the analysis of the data.

TESTS

The low-speed stalling and lift characteristics of the Douglas D-558-II airplane were measured in a series of 1g stall approaches in the following airplane configurations:

1. Basic wing configuration (no fences).

   (a) Slats retracted (locked closed), flaps and landing gear retracted.
   (b) Slats unlocked, flaps and landing gear retracted.
   (c) Slats unlocked, flaps and landing gear extended.

2. Inboard wing fences.

   (a) Slats retracted, flaps and landing gear retracted.
   (b) Slats unlocked, flaps and landing gear retracted.
   (c) Slats unlocked, flaps and landing gear extended.

3. Inboard and outboard wing fences.

   (a) Slats retracted, flaps and landing gear retracted.
   (b) Slats unlocked, flaps and landing gear extended.

4. Wing slats fully extended (no wing fences).

   (a) Flaps and landing gear retracted.
   (b) Flaps and landing gear extended.

5. Wing slats fully extended and inboard wing fences.

   (a) Flaps and landing gear retracted.
   (b) Flaps and landing gear extended.

6. Wing leading-edge chord-extensions (no fences, slats retracted).

   (a) Flaps and landing gear retracted.
   (b) Flaps and landing gear extended.

The stall approaches were performed at altitudes between about 18,700 feet and 21,500 feet and at a generally constant wing loading of 64 pounds per square foot. The location of the airplane center of gravity was between 24.9- and 26.9-percent mean aerodynamic chord for all but the chord-extension configuration. For the chord-extension configuration the center of gravity was located between 22.4- and 22.8-percent mean aerodynamic chord in order to provide the same degree of apparent longitudinal stability for the airplane as in the unmodified configuration with the center of gravity at about 25- to 26-percent mean aerodynamic chord (refs. 3 and 5). Stabilizer control settings ranging from 1.3° to 2.3° were used for all the maneuvers.

In general, the stall-approach maneuvers were performed at a rate of decreasing airspeed of about 1 to 2 miles per hour per second. The pilots attempted to continue the maneuver to as low a speed as feasible, but usually terminated the maneuver after pitch-up or severe roll-off

was experienced and subsequently effected recovery. As a result, the complete wing stall or maximum normal-force coefficient generally was not realized in the maneuvers.

RESULTS AND DISCUSSION

Data obtained during the stall-approach maneuvers performed in each configuration are presented in figures 10 to 23 in the form of time-history plots and as the variation of several pertinent longitudinal stability quantities with indicated airspeed. Inasmuch as almost similar wing loadings and test altitudes existed for all maneuvers, indicated airspeed has been used as a variable to show and compare stability characteristics for the various configurations. For convenience in comparing the data, the flight conditions and figure numbers of the data presented are tabulated in table II. Figures 24 to 27 present comparison plots showing the effect of wing modification on the variation of elevator deflection and normal-force coefficient with angle of attack for each configuration investigated.

Because of the similarity in several of the characteristics exhibited by the airplane during the stall approaches, regardless of wing configuration, a rather complete discussion of the data obtained is confined to the basic wing configuration. Only those characteristics pertinent to each of the other configurations are discussed in this paper. For convenience in presentation, a summary of results obtained during the reported maneuvers is presented in table III.

Effect of Wing Configuration on Stalling and Lift Characteristics

Basic wing configuration.- Measured data obtained during 1g stall approaches performed in each of three conditions with the basic wing configuration are shown in figures 10 to 12. In the clean condition the poor lateral damping characteristics of the airplane for small-amplitude oscillations (ref. 8) are observed at $V_i > 195$ mph; however, below 195 mph the lateral stability improves. Lateral stability again deteriorates at speeds below approximately 190 mph, with accompanying erratic motion in both the aileron and elevator controls (fig. 10(a)). As a result of the erratic control motion and poor airplane response at lower speeds shown in figure 10(a), the variation of the quantities plotted against V_i in figure 10(b) shows appreciable scatter. However, general trends may be noted from these plots. The apparent stick-fixed longitudinal stability, indicated by the slope of the curve of elevator deflection against V_i, appears to be positive as speed is

decreased to $V_i \approx 185$ mph, is approximately neutral to $V_i \approx 170$ mph, and appears unstable at speeds below $V_i \approx 170$ mph. In figure 10(a) a large amount of down-elevator control application is apparent from time 102.0 seconds to 104.3 seconds, after which up-elevator control application is again apparent. This trend results from the apparent pitch-up experienced by the pilot, who applied excessive elevator-control deflections in an attempt to control the airplane, thereby causing the airplane to pitch down and then up. Subsequent to this experience the maneuver was terminated. The push-down performed by the pilot usually accentuated the stick-fixed instability of the airplane at low speeds. (This general trend was experienced and followed by the pilots during most of the maneuvers, as may be noted in the data presented herein.) In general, the apparent stick-free longitudinal stability, indicated by the slope of the curve of F_e against V_i, appears neutral over most of the stall-approach maneuver and much of the elevator-force variation lies within the control-friction band (fig. 9). Peak values of $\alpha \approx 14^\circ$ and $C_{N_A} \approx 0.95$, corresponding to a minimum speed of $V_i = 168$ mph, were obtained in this maneuver.

With the slats unlocked appreciable aileron control movement was required as the stall was approached, but the airplane motions appear relatively smooth (fig. 11). The opening of the slat appears gradual and smooth and the airplane appears to retain apparent stick-fixed longitudinal stability down to $V_i \approx 175$ mph. Opening the slat had no effect on the speed at which the airplane became unstable ($V_i \approx 170$ mph); however, higher peak values of α and C_{N_A} and a lower minimum speed were realized with the slats unlocked. The apparent stick-free longitudinal stability appeared neutral over most of the stall-approach maneuver and unstable at speeds below $V_i \approx 178$ mph.

Extending the flaps and landing gear with the slats unlocked increased the degree of apparent stick-fixed and stick-free longitudinal stability at comparable airspeeds and appreciably decreased the minimum speed and increased the peak values of α and C_{N_A} attained (fig. 12). Stick-fixed instability is apparent at speeds below $V_i \approx 144$ mph. Stick-free instability is apparent at speeds below $V_i \approx 147$ mph. In general, the slat opening was smooth and gradual and, as the stall was approached, the control motions and airplane response appear smoother than in the other two flight conditions discussed. At $V_i > 180$ mph, however, a Dutch roll type of oscillation was experienced and is shown in the data of figure 12(a). In addition some evidence of right-wing heaviness, resulting from extending the flaps and landing gear, is shown by a comparison of the δ_a data of figures 10(a), 11(a), and 12(a).

Unlocking the slats with gear and flaps retracted produced no increment of C_{N_A} for given values of α; however, extending the flaps and gear produced an increment in C_{N_A} of about 0.3.

Pilots' descriptions of the stall-approach maneuvers in the subject configuration are in general agreement with the preceding discussion. In addition, the pilots detected the onset of mild buffet at $V_i \approx 190$ mph in stalls performed with flaps and gear retracted, and at $V_i \approx 170$ mph with the flaps and gear extended and slats unlocked.

Configuration with inboard wing fences.- Data obtained during 1 g stall approaches performed with inboard wing fences installed are presented in figures 13 to 15. A more complete discussion of stall-approach maneuvers performed in this configuration with another D-558-II airplane is presented in reference 9.

Adding the inboard wing fences caused a slight improvement in the dynamic lateral stability characteristics of the airplane in the clean condition and made possible considerably steadier flight. In addition the airplane tended to retain some degree of apparent stick-fixed longitudinal stability to lower airspeeds with inboard fences than was maintained in the basic wing configuration. (Compare data of figs. 10 and 13; also see table III.) However, with the addition of the wing fences, wing dropping was experienced near the stall as evidenced by the left aileron input starting at time 12 seconds (fig. 13(a)) and as reported by the pilot.

Unlocking the slats had a small effect toward increasing the degree of stick-fixed stability exhibited by the airplane in the stall approach and lowered the speed below which the airplane became stick-fixed unstable to $V_i \approx 161$ mph (fig. 14). The latter effect is in agreement with the results of the wind-tunnel investigation of reference 4 and was also reported in greater detail in reference 9. Also, as previously discussed for the basic wing configuration, the pilot reported that unlocking the slats resulted in a smoother stall-approach maneuver in this configuration than with slats locked closed. As a result of the improved stalling characteristics, a lower minimum speed and higher peak values of α and C_{N_A} were attained in this maneuver than were obtained with the basic wing configuration.

With the slats unlocked and flaps and landing gear extended, a Dutch roll oscillation was experienced at the higher stall-approach speeds. Erratic control motions and airplane response were exhibited at the lower speeds and the airplane motion and elevator input appeared 180° out of phase prior to the stall (fig. 15(a)). The degree of apparent stick-fixed stability was approximately the same with the slats

unlocked and flaps and gear retracted or extended at comparably low and moderate values of α, but at comparable speeds appeared to be greater with flaps and gear extended. In other respects the airplane exhibited roughly the same characteristics as in the basic wing configuration. Buffet warning was reported by the pilot at $V_i \approx 155$ mph which is well above the stall speed. The pilot also reported the lateral stability was marginal below about 160 mph.

Configuration with inboard and outboard wing fences.- Data obtained during 1g stall-approach maneuvers performed in the configuration incorporating two fences in the clean and landing conditions are shown in figures 16 and 17.

For the clean-condition stall approach a small degree of apparent stick-fixed longitudinal stability is exhibited at speeds down to $V_i \approx 175$ mph. Below $V_i \approx 175$ mph the static longitudinal stability appeared to decrease and the pilot experienced difficulty in flying the airplane smoothly. These effects may be noted in figure 16, particularly the erratic airplane and control motions as the stall was approached.

Extending the flaps and gear and unlocking the slats resulted in an increase in the apparent stick-fixed longitudinal stability at comparable speeds (fig. 17). In general, the stick-free stability was neutral at speeds above $V_i \approx 145$ mph. Below $V_i \approx 145$ mph the apparent stick-free and stick-fixed stability appeared to decrease. Evaluation of this condition, however, is difficult because of the erratic airplane and control motions in this speed range. Slat opening appears fairly gradual and smooth and pilot observation of buffet was reported at $V_i \approx 143$ mph, which is fairly close to the minimum speed of 131 mph indicated for this maneuver.

In general this configuration, as did the previous configuration, provided only a small improvement in handling characteristics compared with the characteristics of the basic wing configuration.

Configuration with slats fully extended (no wing fences).- Stall-approach data obtained with the slats in the fully extended position (fig. 5) and with no wing fences installed are shown in figures 18 and 19 for the conditions with flaps and gear retracted and extended, respectively.

In either condition, the data show the control motions and airplane motions to be erratic as the minimum speed of each maneuver was approached. A comparison of the data of figures 18 and 19 and table III shows that the airplane exhibited a greater degree of apparent stick-fixed stability in the landing condition and retained stability down to appreciably lower speeds than when the flaps and gear were retracted. In both conditions the stick-free characteristics appear marginal over most of the speed

range and unstable at the lower speeds. With flaps and gear retracted the pilot reported roll-off tendencies near minimum speed. With flaps and gear extended, marginal dynamic lateral stability was reported at speeds below $V_i \approx 150$ mph and the data of figure 19(a) indicate a left-wing heaviness as the speed decreased.

With the slats fully extended the airplane attained appreciably higher values of α and C_{N_A} and a lower minimum speed than in the basic wing configuration when the flaps and gear were retracted. These margins were not so marked, however, in the landing condition. In most other respects these two configurations appeared similar.

Configuration with slats fully extended and inboard wing fences.- Data obtained during the 1g stall-approach maneuvers with slats fully extended and inboard fences at 0.36 wing semispan are shown in figure 20 for the condition with flaps and gear retracted and in figure 21 for the landing condition.

The control motions and airplane response appear only slightly erratic with flaps and landing gear retracted (fig. 20(a)); however, this effect is mainly in the lateral plane. Appreciable use of aileron and rudder is noted in the time-history plot for the landing condition (fig. 21(a)), but the airplane motions do not appear severe until the stall is approached. With flaps and gear retracted, the airplane is shown to be slightly stable longitudinally to $V_i \approx 167$ mph as speed is reduced, neutrally stable to 160 mph, and apparently unstable at lower speeds. With flaps and gear extended the degree of apparent stability exhibited at comparable speeds or angles of attack was generally greater than with flaps and gear retracted. Also in the landing condition the airplane retained stability to the lowest speed attained ($V_i = 127$ mph), although a marginal region is apparent from $V_i \approx 145$ mph to 135 mph. Adequate stall warning in the form of buffet became more apparent as the stall was approached in either flight condition.

Because of the retention of apparent stick-fixed stability to lower speeds in the landing condition and the absence of any pitch-up, this configuration was considered by the pilots to be an improvement over the basic wing configuration at the lower speeds. Table III also shows that this configuration generally provided some increase in peak α and C_{N_A} and a decrease in minimum V_i attained.

Wing leading-edge chord-extension configuration.- Data obtained during 1g stall-approach maneuvers performed in the clean and landing conditions with wing leading-edge chord-extensions installed over the outer 0.32 semispan of each wing panel are presented in figures 22 and 23, respectively.

Inspection of the data of figure 22 shows that the stall performed in the clean condition was generally smooth, with rolling oscillations occurring at speeds below $V_i \approx 185$ mph as the stall was approached. The apparent stick-fixed stability was generally stable down to $V_i \approx 197$ mph, neutrally stable between $V_i \approx 197$ mph and 170 mph, and unstable below $V_i = 170$ mph. The stick-free stability was generally neutral at speeds above 175 mph and unstable at lower speeds. In the landing condition a slight rolling oscillation was apparent during the entire maneuver and became more severe near minimum speeds(fig. 23(a)). At $V_i < 200$ mph the apparent stick-fixed stability was appreciably greater in the landing condition than in the clean condition and positive stability was retained to the minimum speed of the maneuver in the landing condition. However, the pilot reported some tendency toward longitudinal and lateral instability in the landing condition at minimum speed, and the data of figure 23(a) indicate this trend. Also, the stick-free stability in the landing condition was greater than in the clean condition (compare figs. 23(a) and 22(a)). The peak values of α and C_{N_A} attained in the landing condition were not appreciably higher than in the clean condition, as had been experienced in other configurations investigated, but the incremental effect on C_{N_A} values over the α range was the same as experienced with other configurations. These effects resulted from the fact that the slats were retracted for this configuration, hence wing-flow separation probably tended to occur at a lower value of α when the flaps were extended. Also, the pilot noted the start of buffeting at slightly lower values of α and C_{N_A} for this configuration than for other configurations tested and the buffet intensity rise appeared more severe at given values of α and C_{N_A}. Therefore, the maneuver in the landing condition was terminated at a lower level of α.

Comparison of Stalling and Lift Characteristics With Various Wing Modifications

Flaps and landing gear retracted.- The effect of the various wing stall-control devices on the stability and lift characteristics of the Douglas D-558-II airplane in the clean condition is shown in figure 24. Addition of wing fences or the chord-extension to the wing panels had little or no effect on the variation of normal-force coefficient with angle of attack, except for a slight decrease in the slope at $\alpha > 12^\circ$ for the one-fence and chord-extension configurations. Also, the values of peak normal-force coefficient attained were about the same for the configurations compared in figure 24. An appreciable difference in the apparent stability characteristics, as determined by the slope of the curve of δ_e plotted against α, is exhibited for the configurations

discussed. The basic wing configuration exhibits about the same degree of apparent stability up to $\alpha \approx 10^{\circ}$ as exhibited by the two-fence and chord-extension configurations up to $\alpha \approx 9^{\circ}$. This degree of stability is greater than for the one-fence configuration. However, the basic wing configuration appears unstable at $\alpha \gtrapprox 12^{\circ}$, whereas the other configurations appear unstable at $\alpha \gtrapprox 13^{\circ}$.

The effects on the airplane stability and lift characteristics of unlocking the slats so they were free to float, and of locking the slats in the fully extended position, are shown in figure 25 for the condition of flaps and gear retracted. The slats had little or no effect on the slopes of the curves of normal-force coefficient plotted against angle of attack, regardless of the wing-fence configuration. The peak values of C_{N_A} attained were appreciably larger when the slats were free floating and to a greater degree when the slats were fully extended. These higher values of peak C_{N_A} result from the effectiveness of the slats in delaying separation and extending the stable region of the airplane to lower speeds and to higher angles of attack. Comparison of the curves of δ_e plotted against α in figure 25 indicates that the free-floating slats and the fully extended slats generally had an inconsistent or negligible effect on the degree of stability exhibited in the stable region, but extended the peak angle for the positive stability range from $\alpha \approx 10^{\circ}$ (with slats retracted) to $\alpha \approx 12^{\circ}$ for the basic wing airplane, and from $\alpha \approx 13^{\circ}$ to $\alpha \approx 15^{\circ}$ for the inboard wing-fence configuration. Regardless of slat configuration, the data show the airplane becomes unstable at a greater value of α when the inboard wing fence is installed. These results are in general agreement with those shown in the wind-tunnel investigation of reference 4 for the effects of wing fences and slats on stability. It is noteworthy that the position of the free-floating slats above $\alpha \approx 13^{\circ}$ was similar to the fully extended slat position (figs. 11 and 14), therefore the airplane exhibited generally similar characteristics at the higher values of α when the slats were free floating or fully extended.

Flaps and landing gear extended.- With the flaps and gear extended, addition of wing fences with the slats unlocked or addition of wing chord-extensions (slats retracted) had a negligible effect on the variation of C_{N_A} with α, except for a decrease in slope exhibited at $\alpha > 12^{\circ}$ for the inboard-fence configuration (fig. 26). Peak values of C_{N_A} attained with the basic wing configuration and with both wing-fence configurations were approximately the same. The appreciably lower peak value of C_{N_A} for the chord-extension configuration probably results from the fact that the wing slats were retracted for this configuration and earlier and more severe buffeting was detected by the pilot who terminated the maneuver at a lower value of α and C_{N_A} than for the other configurations tested. The degree of apparent stability exhibited by the

four configurations compared in figure 26 does not differ appreciably at the more moderate values of α, except possibly for the slightly greater apparent stability exhibited by the chord-extension configuration. At angles of attack above about 10° or 12° all configurations show a neutrally stable region for several degrees, followed by an unstable region for the basic wing configuration and both fence configurations. Because of the approximately neutrally stable region apparent at the higher values of α, appreciable elevator-control movements were made by the pilot during some stall maneuvers with some erratic response from the airplane, resulting in the scatter in data points shown in figure 26.

Inasmuch as 1 g stall-approach maneuvers were not performed with the slats retracted and flaps and gear extended, a comparison of only the effects of the free-floating slat and the fully extended slat on airplane lift and stability characteristics in the landing condition is feasible. A comparison of data for these configurations is shown in figure 27 for both the basic wing and inboard-fence configurations. A slight increase in the normal-force-coefficient slope at the lower values of α for both extended-slat configurations is apparent compared with the data for the free-floating slat configurations. At the higher angles of attack, however, the variation of C_{N_A} with α is greater for the inboard-fence configuration when the slats are fully extended, and is greater for the basic wing configuration when the slats are free floating (unlocked). The reasons for these differences are not readily apparent, especially since the free-floating slats are essentially "fully extended" at angles of attack above about 12° (figs. 12(a) and 15(a)). Slat configuration appeared to have only a small effect on the apparent stability characteristics at $\alpha \lessapprox 12^\circ$ for either wing-fence condition; however, it will be noted that the airplane appeared somewhat more stable with no wing fences than with the inboard fences when the slats were fully extended. At $\alpha \gtrapprox 12^\circ$ the main effect noted is the unstable trend shown for the basic wing slats-extended configuration as compared to the generally neutrally stable or slightly stable regions shown by the other configurations. This effect is in agreement with the results shown in reference 4 for the effects of adding similar inboard wing fences to the extended-slat airplane configuration.

In general, the pilots considered the configuration embodying extended wing slats and inboard wing fences the most satisfactory for performing stall-approach maneuvers.

CONCLUDING REMARKS

The low-speed stalling and lift characteristics of the Douglas D-558-II airplane were measured in a series of 1 g stall-approach maneuvers

performed with several wing modifications designed to alleviate swept-wing instability and pitch-up. The various airplane configurations investigated include a basic wing configuration and two wing-fence configurations in combination with retracted, free-floating, or extended slats, and a wing leading-edge chord-extension configuration. All configurations were investigated with flaps and landing gear retracted and extended.

With slats, flaps, and landing gear retracted, none of the wing modifications investigated had an appreciable effect on the lift or stability characteristics at low and moderate angles of attack. Regardless of wing-fence configuration, appreciably larger values of peak normal-force coefficient were attained with slats unlocked (free floating) or fully extended than with slats closed. Wing fences and the chord-extension tended to delay the onset of instability with slats retracted, and the stable region was further extended for the configurations with either no wing fences or inboard wing fences when the slats were free floating or extended.

With flaps and landing gear extended, only the fully extended slat configuration affected the variation of normal-force coefficient with angle of attack by increasing this variation slightly. Peak values of normal-force coefficient attained were the same for all configurations except the chord-extension configuration for which excessive buffeting caused earlier termination of the maneuver. Most of the configurations had little or no effect on the stability characteristics over most of the lower and moderate angle-of-attack range. The airplane appeared somewhat more stable, however, with no wing fences installed than with wing fences installed when the slats were extended. At larger angles of attack and with slats extended, inboard wing fences materially improved the stability characteristics of the airplane.

At any given angle of attack, extending the flaps provided an increment in normal-force coefficient of about 0.3; whereas, except for the larger angles of attack, the free-floating or fully extended slats provided no incremental lift. The airplane generally appeared more stable longitudinally at comparable speeds with the flaps deflected than with flaps retracted; however, marginal dynamic lateral stability was evident for several configurations with the flaps extended or retracted.

In general, adequate stall warning in the form of buffeting was noted by the pilot well above minimum speed and in the stable flight

region of the airplane, particularly for the chord-extension configuration for which buffeting appeared aggravated.

High-Speed Flight Station,
National Advisory Committee for Aeronautics,
Edwards, Calif., May 18, 1955.

REFERENCES

1. Fischel, Jack, and Nugent, Jack: Flight Determination of the Longitudinal Stability in Accelerated Maneuvers at Transonic Speeds for the Douglas D-558-II Research Airplane Including the Effects of an Outboard Wing Fence. NACA RM L53A16, 1953.

2. Fischel, Jack: Effect of Wing Slats and Inboard Wing Fences on the Longitudinal Stability Characteristics of the Douglas D-558-II Research Airplane in Accelerated Maneuvers at Subsonic and Transonic Speeds. NACA RM L53L16, 1954.

3. Fischel, Jack, and Brunn, Cyril D.: Longitudinal Stability Characteristics in Accelerated Maneuvers at Subsonic and Transonic Speeds of the Douglas D-558-II Research Airplane Equipped With a Leading-Edge Wing Chord-Extension. NACA RM H54H16, 1954.

4. Queijo, M. J., and Jaquet, Byron M.: Wind-Tunnel Investigation of the Effect of Chordwise Fences on Longitudinal Stability Characteristics of an Airplane Model With a 35° Sweptback Wing. NACA RM L50K07, 1950.

5. Jaquet, Byron M.: Effects of Chord Discontinuities and Chordwise Fences on Low-Speed Static Longitudinal Stability of an Airplane Model Having a 35° Sweptback Wing. NACA RM L52C25, 1952.

6. Jaquet, Byron M.: Effects of Chord-Extension and Droop of Combined Leading-Edge Flap and Chord-Extension on Low-Speed Static Longitudinal Stability Characteristics of an Airplane Model Having a 35° Sweptback Wing With Plain Flaps Neutral or Deflected. NACA RM L52K21a, 1953.

7. Gracey, William, Letko, William, and Russell, Walter R.: Wind-Tunnel Investigation of a Number of Total-Pressure Tubes at High Angles of Attack - Subsonic Speeds. NACA TN 2331, 1951. (Supersedes NACA RM L50G19.)

8. Stillwell, W. H., and Wilmerding, J. V.: Flight Measurements With the Douglas D-558-II (BuAero No. 37974) Research Airplane - Dynamic Lateral Stability. NACA RM L51C23, 1951.

9. Stillwell, W. H., Wilmerding, J. V., and Champine, R. A.: Flight Measurements With the Douglas D-558-II (BuAero No. 37974) Research Airplane - Low-Speed Stalling and Lift Characteristics. NACA RM L50G10, 1950.

TABLE I.- PHYSICAL CHARACTERISTICS OF THE UNMODIFIED DOUGLAS D-558-II AIRPLANE

Wing:	
Root airfoil section (normal to 0.30 chord of unswept panel)	NACA 63-010
Tip airfoil section (normal to 0.30 chord of unswept panel)	NACA 63_1-012
Total area, sq ft	175.0
Span, ft	25.0
Mean aerodynamic chord, in.	87.301
Root chord (parallel to plane of symmetry), in.	108.51
Tip chord (parallel to plane of symmetry), in.	61.18
Taper ratio	0.565
Aspect ratio	3.570
Sweep at 0.30 chord of unswept panel, deg	35.0
Sweep of leading edge, deg	38.8
Incidence at fuselage center line, deg	3.0
Dihedral, deg	-3.0
Geometric twist, deg	0
Total aileron area (rearward of hinge line), sq ft	9.8
Aileron travel (each), deg	±15
Total flap area, sq ft	12.58
Flap travel, deg	50
Horizontal tail:	
Root airfoil section (normal to 0.30 chord of unswept panel)	NACA 63-010
Tip airfoil section (normal to 0.30 chord of unswept panel)	NACA 63-010
Area (including fuselage), sq ft	39.9
Span, in.	143.6
Mean aerodynamic chord, in.	41.75
Root chord (parallel to plane of symmetry), in.	53.6
Tip chord (parallel to plane of symmetry), in.	26.8
Taper ratio	0.50
Aspect ratio	3.59
Sweep at 0.30 chord line of unswept panel, deg	40.0
Dihedral, deg	0
Elevator area, sq ft	9.4
Elevator travel, deg	
Up	25
Down	15
Stabilizer travel, deg	
Leading edge up	4
Leading edge down	5
Vertical tail:	
Airfoil section (normal to 0.30 chord of unswept panel)	NACA 63-010
Area, sq ft	36.6
Height from fuselage center line, in.	98.0
Root chord (parallel to fuselage center line), in.	146.0
Tip chord (parallel to fuselage center line), in.	44.0
Sweep angle at 0.30 chord of unswept panel, deg	49.0
Rudder area (rearward of hinge line), sq ft	6.15
Rudder travel, deg	±25
Fuselage:	
Length, ft	42.0
Maximum diameter, in.	60.0
Fineness ratio	8.40
Speed-retarder area, sq ft	5.25
Engines:	
Turbojet	J34-WE-40
Rocket	LR8-RM-6
Airplane weight, lb:	
Full jet and rocket fuel	15,570
Full jet fuel	12,382
No fuel	10,822

TABLE II.- INDEX TO DATA FIGURES

(a) Complete data for each stall-approach maneuver

Airplane configuration	Slat configuration	Flaps and landing gear	Figure number
Basic wing (no fences)	Retracted Unlocked Unlocked	Retracted Retracted Extended	10(a) and 10(b) 11(a) and 11(b) 12(a) and 12(b)
Inboard wing fences	Retracted Unlocked Unlocked	Retracted Retracted Extended	13(a) and 13(b) 14(a) and 14(b) 15(a) and 15(b)
Inboard and outboard wing fences	Retracted Unlocked	Retracted Extended	16(a) and 16(b) 17(a) and 17(b)
Wing slats fully extended (no wing fences)	Extended Extended	Retracted Extended	18(a) and 18(b) 19(a) and 19(b)
Wing slats fully extended and inboard wing fences	Extended Extended	Retracted Extended	20(a) and 20(b) 21(a) and 21(b)
Wing leading-edge chord-extensions	Retracted Retracted	Retracted Extended	22(a) and 22(b) 23(a) and 23(b)

TABLE II.- INDEX TO DATA FIGURES - Concluded

(b) Comparison data of lift and stability characteristics

Airplane configuration	Slat configuration	Flaps and landing gear	Figure number
Basic wing (no fences)	Retracted	Retracted	24
Inboard wing fences	Retracted	Retracted	24
Inboard and outboard wing fences	Retracted	Retracted	24
Wing leading-edge chord-extensions	Retracted	Retracted	24
Basic wing (no fences)	Retracted	Retracted	25
	Unlocked	Retracted	25
	Extended	Retracted	25
Inboard wing fences	Retracted	Retracted	25
	Unlocked	Retracted	25
	Extended	Retracted	25
Basic wing (no fences)	Unlocked	Extended	26
Inboard wing fences	Unlocked	Extended	26
Inboard and outboard wing fences	Unlocked	Extended	26
Wing leading-edge chord-extensions (no slats)	Unlocked	Extended	26
Basic wing (no fences)	Unlocked	Extended	27
	Extended	Extended	27
Inboard wing fences	Unlocked	Extended	27
	Extended	Extended	27

TABLE III.- SUMMARY OF RESULTS OBTAINED DURING STALL APPROACHES OF THE DOUGLAS D-558-II RESEARCH AIRPLANE

Airplane configuration	Slat configuration	Flaps and landing gear	Apparent longitudinal stability						Pilot report of onset of buffeting, V_i, mph	Peak α, deg	Peak C_{N_A}	Minimum V_i, mph	Remarks
			Stick-fixed			Stick-free							
			Stable	Neutral	Unstable	Stable	Neutral	Unstable					
Basic wing	Retracted	Retracted	$V_i \geq 185$	$V_i \geq 170$	$V_i \leq 170$	--------	Most of maneuver	--------	190	14.0	0.95	168	Lateral stability deteriorates at $V_i < 192$ mph. Dutch roll oscillation at $V_i > 200$ mph.
	Unlocked	Retracted	$V_i \geq 175$	$V_i \geq 170$	$V_i \leq 170$	--------	Most of maneuver	$V_i \leq 178$	190	15.8	1.02	159	Smooth maneuver.
	Unlocked	Extended	$V_i \geq 145$	----------	$V_i \leq 144$	$V_i \geq 155$	---------	$V_i \leq 147$	170	16.5	1.43	140	Dutch roll oscillation at $V_i > 180$ mph. Right-wing heaviness as stall approached.
Inboard wing fences	Retracted	Retracted	$V_i \geq 175$	----------	$V_i \leq 172$	--------	Most of maneuver	$V_i \leq 175$	200	16.0	0.95	164	Wing dropping as stall approached.
	Unlocked	Retracted	$V_i \geq 161$	----------	$V_i \leq 161$	$V_i \geq 186$	---------	$V_i \leq 186$	Unavailable	17.6	1.12	150	Smooth maneuver.
	Unlocked	Extended	$V_i \geq 131$	----------	$V_i \leq 131$	--------	Most of maneuver	--------	155	23.6	1.44	129	Dutch roll oscillation at higher speeds. Dynamic lateral stability marginal at $V_i < 160$ mph. Right-wing heaviness as stall approached.
Inboard and outboard wing fences	Retracted	Retracted	$V_i \geq 175$	----------	--------	--------	---------	--------	190	14.3	0.98	160	Erratic control and response as stall approached. Apparent stick-fixed longitudinal stability appeared to decrease at $V_i \leq 175$ mph. F_e erratic over entire maneuver.
	Unlocked	Extended	$V_i \geq 143$	----------	--------	$V_i \geq 180$	$V_i \geq 145$	--------	143	18.5	1.40	131	Erratic control and response at $V_i < 145$ mph. Left-wing heaviness as stall approached.
Slats fully extended (no wing fences)	Extended	Retracted	$V_i \geq 185$	----------	$V_i \leq 167$	--------	Most of maneuver	--------	[a]150	19.4	1.19	146	Erratic control and response as stall approached. Roll-off tendency near minimum speed.
	Extended	Extended	$V_i \geq 149$	----------	$V_i \leq 149$	--------	---------	$V_i \leq 150$	[a]145	19.3	1.42	132	Erratic control and response as stall approached. Lateral stability marginal at $V_i < 150$ mph. Left-wing heaviness as stall approached.
Slats fully extended and inboard wing fences	Extended	Retracted	$V_i \geq 167$	$V_i \geq 160$	$V_i \leq 160$	$V_i \geq 169$	---------	$V_i \leq 169$	184	18.3	1.17	149	
	Extended	Extended	$V_i \geq 127$	$145 > V_i > 135$	--------	--------	Most of maneuver	--------	147	18.7	1.43	127	
Wing leading-edge chord-extensions	Retracted	Retracted	$V_i \geq 197$	$V_i \geq 170$	$V_i \leq 170$	--------	$V_i \geq 175$	$V_i \leq 175$	200	15.0	0.98	161	Rolling oscillation at $V_i \leq 185$ mph.
	Retracted	Extended	To minimum speed	----------	--------	$V_i \geq 155$	---------	$V_i \leq 155$	160	11.8	1.12	152	Rolling oscillation during entire maneuver. Right-wing heaviness.

[a]Pilot report of heavy buffeting.

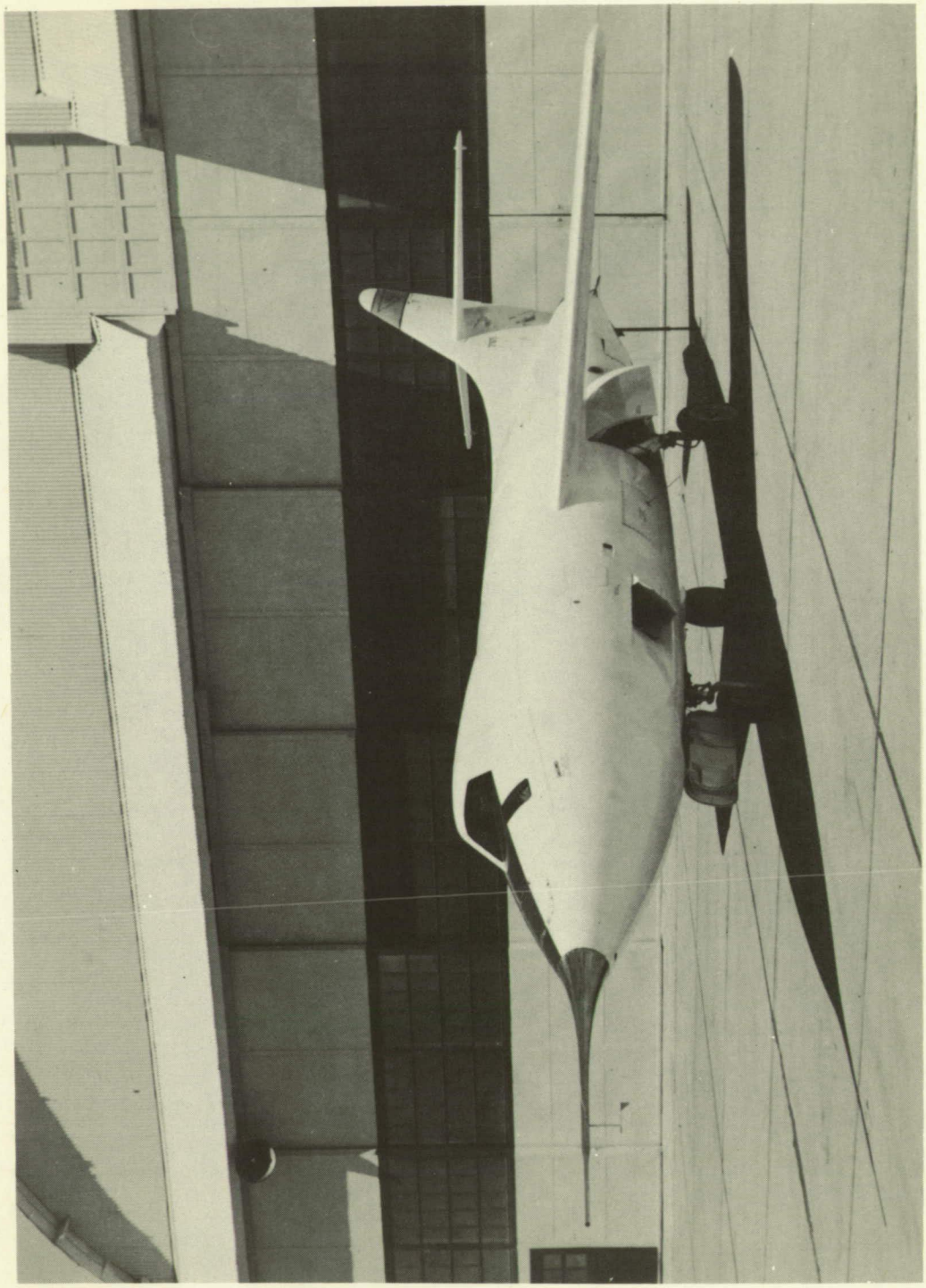

L-87973

Figure 1.- Three-quarter front view of Douglas D-558-II airplane.

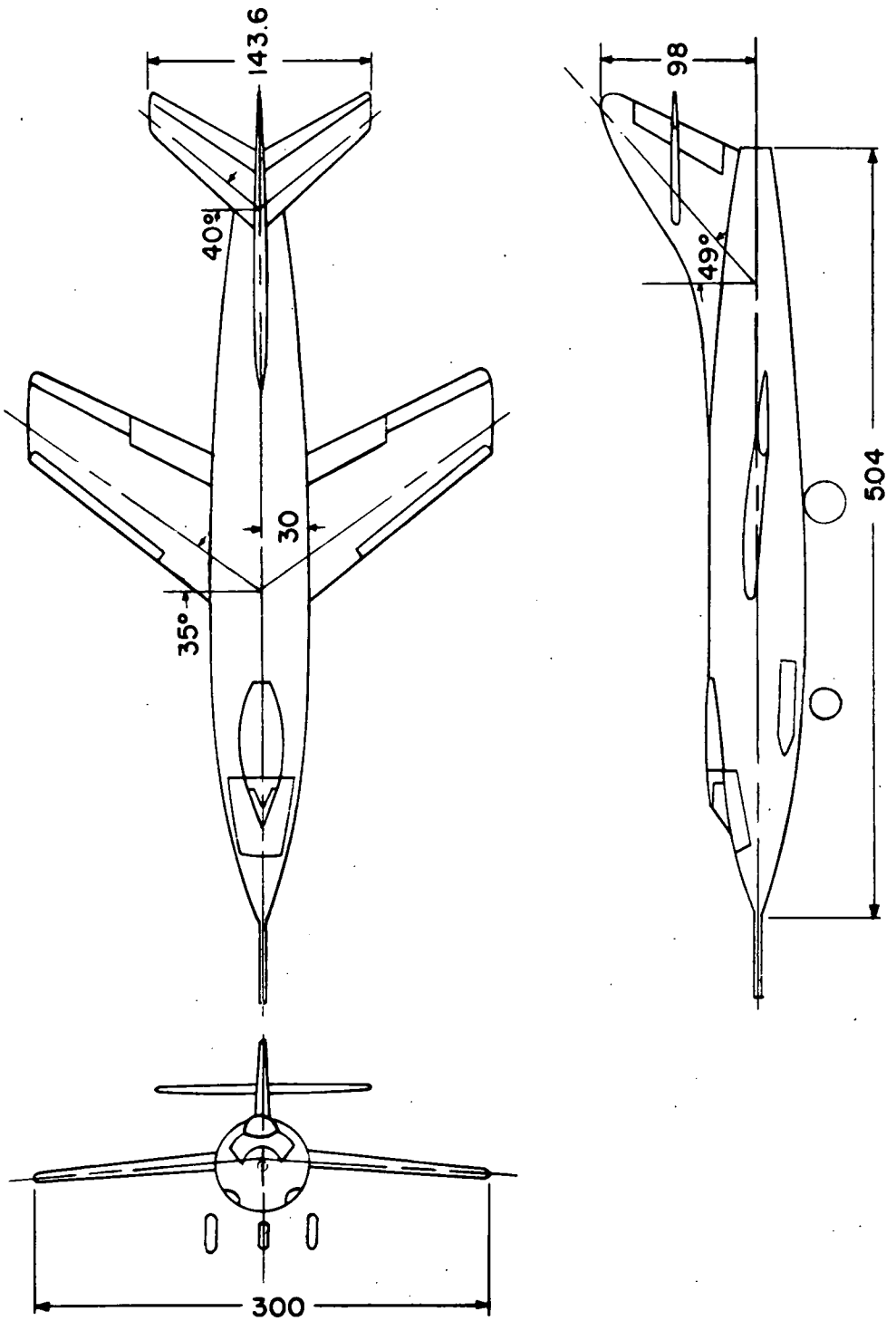

Figure 2.- Three-view drawing of the Douglas D-558-II research airplane. All dimensions in inches.

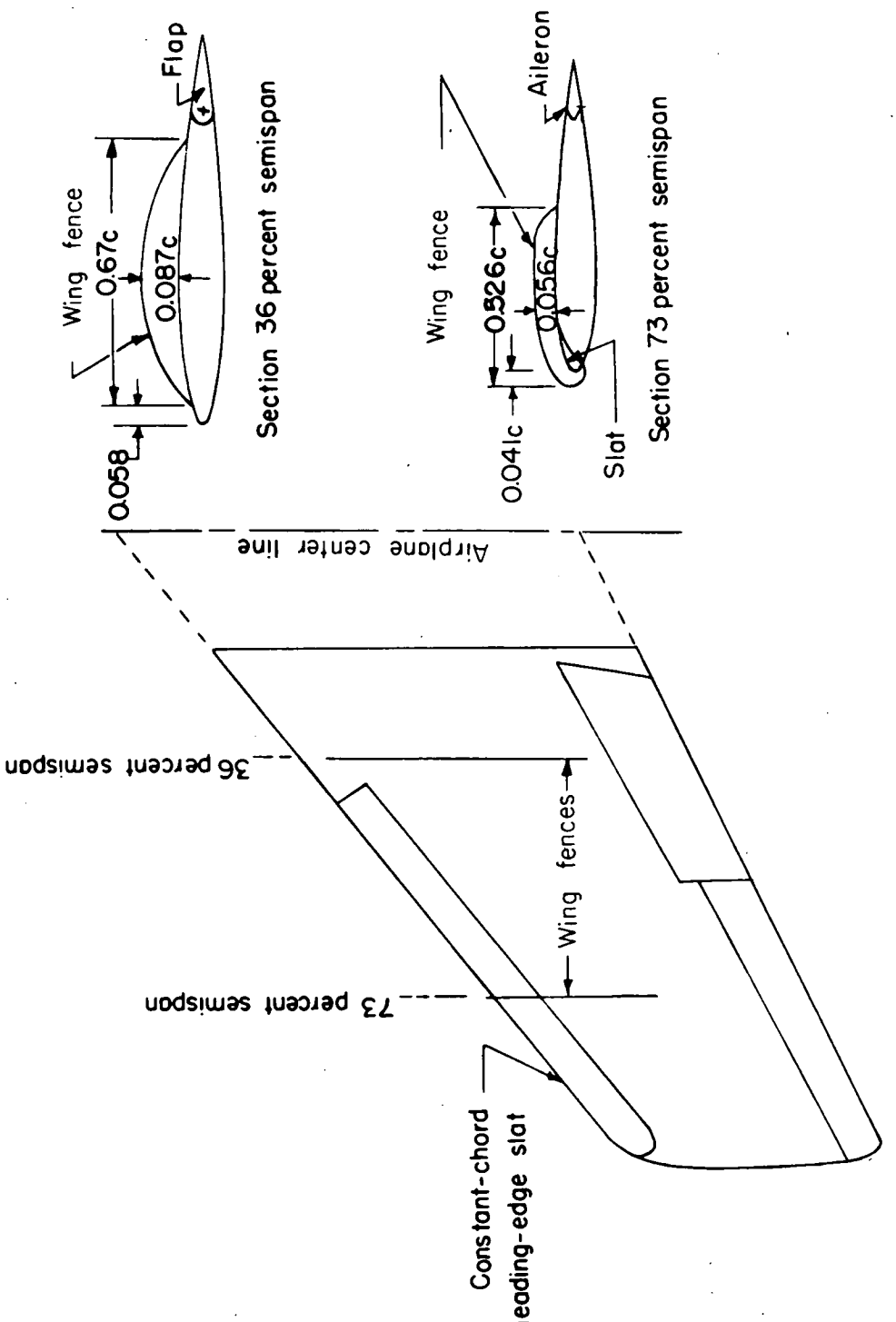

Figure 3.- Plan form and sections of the wing of the D-558-II airplane showing the location and shape of wing fences (stall-control vanes) used in the investigation.

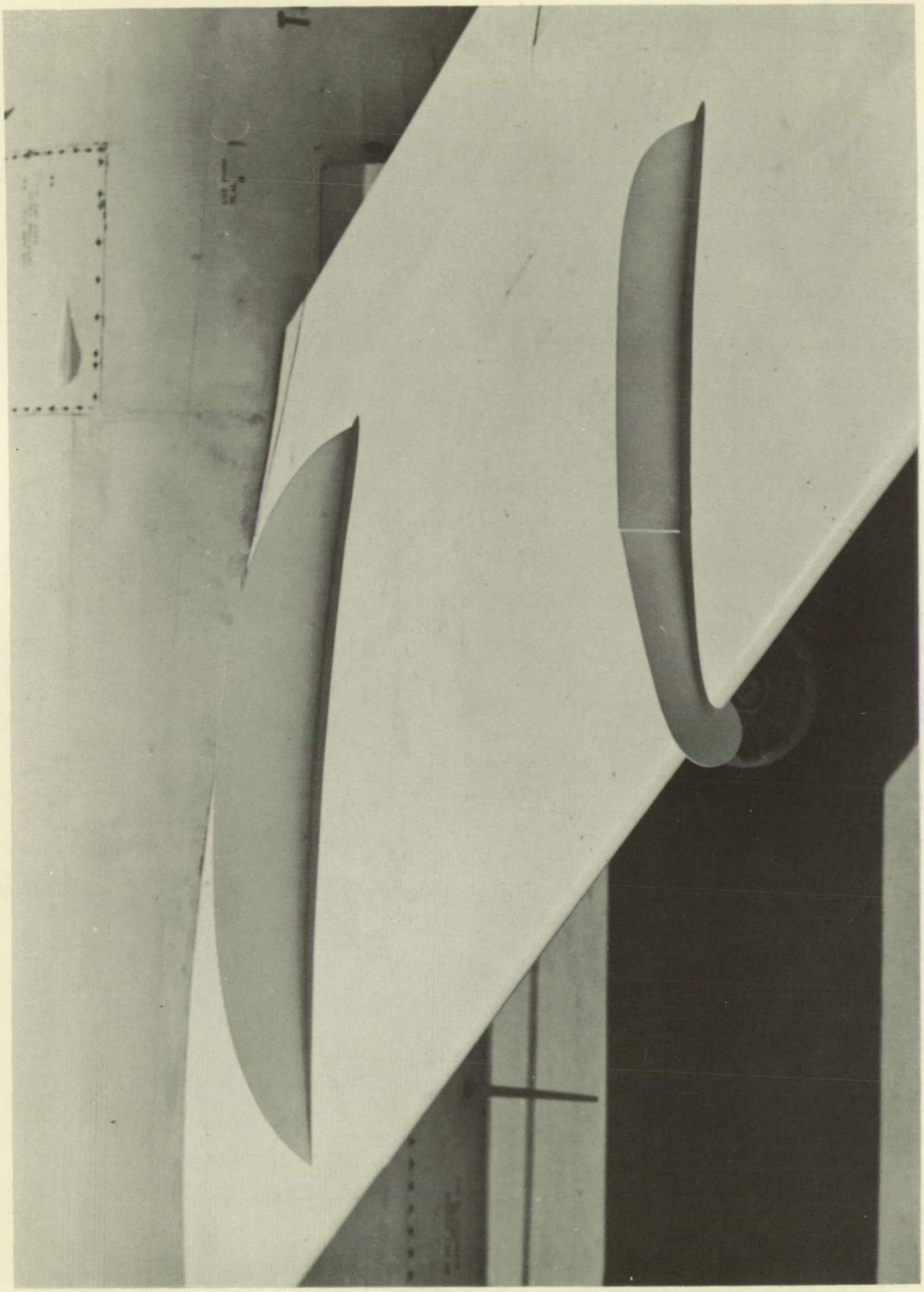

L-87974

Figure 4.- Photograph of the D-558-II wing, showing the inboard and outboard fences (stall-control vanes) on the wing.

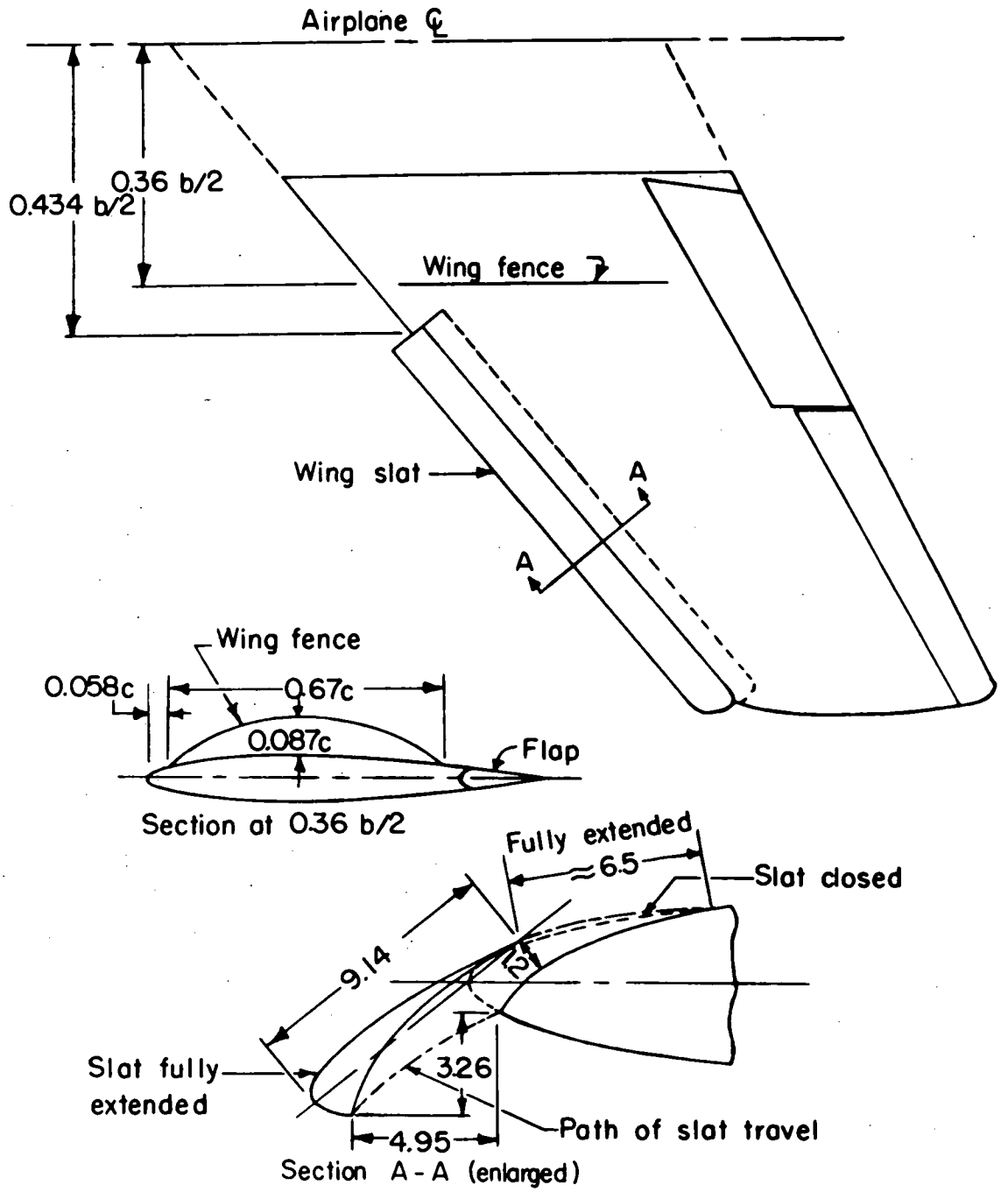

Figure 5.- Plan form and sections of the wing of the D-558-II airplane showing details of the wing slat in the retracted and extended positions.

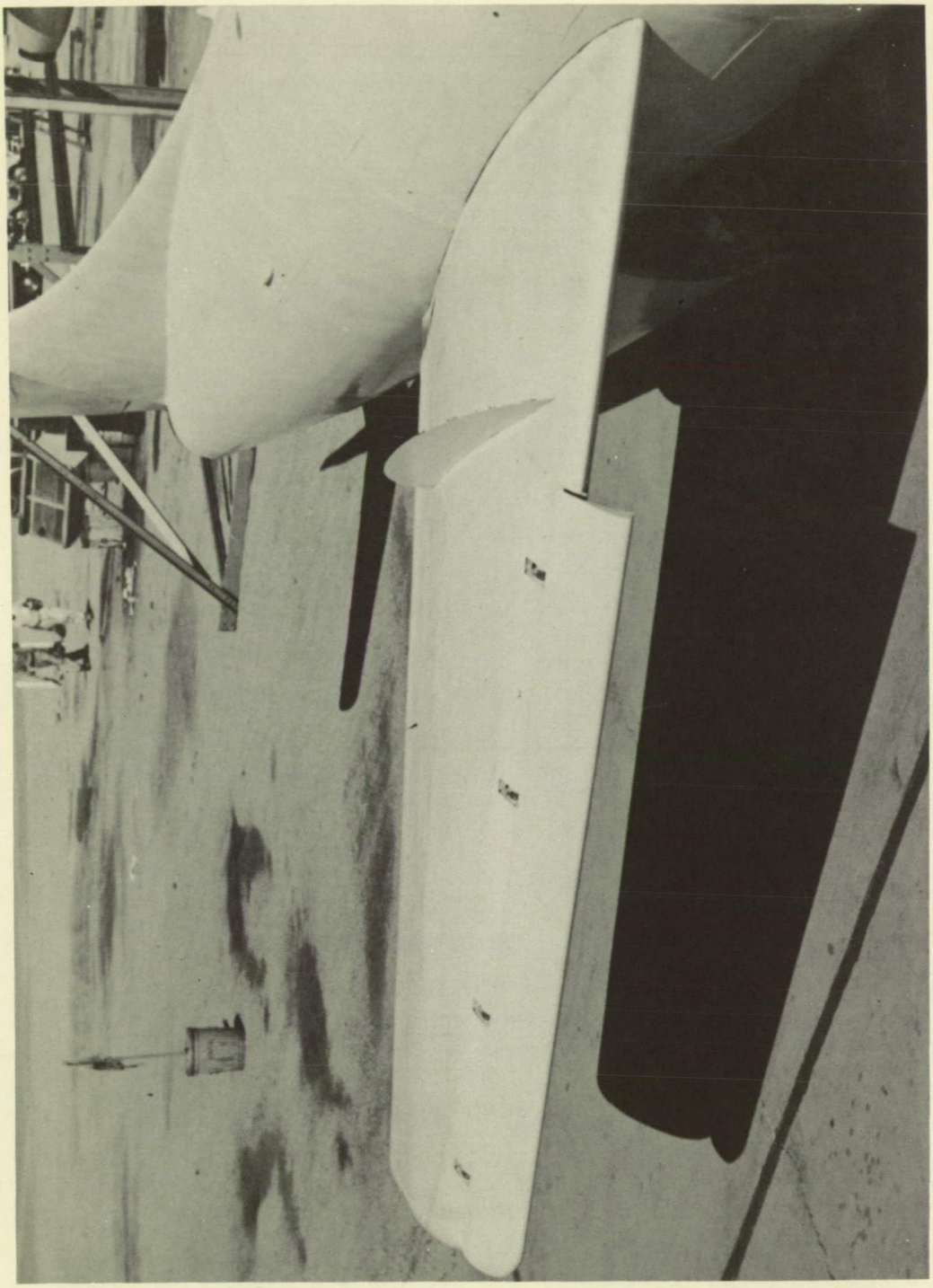

L-87975

Figure 6.- Photograph of right wing of D-558-II airplane showing slat in fully extended position and inboard fence on wing.

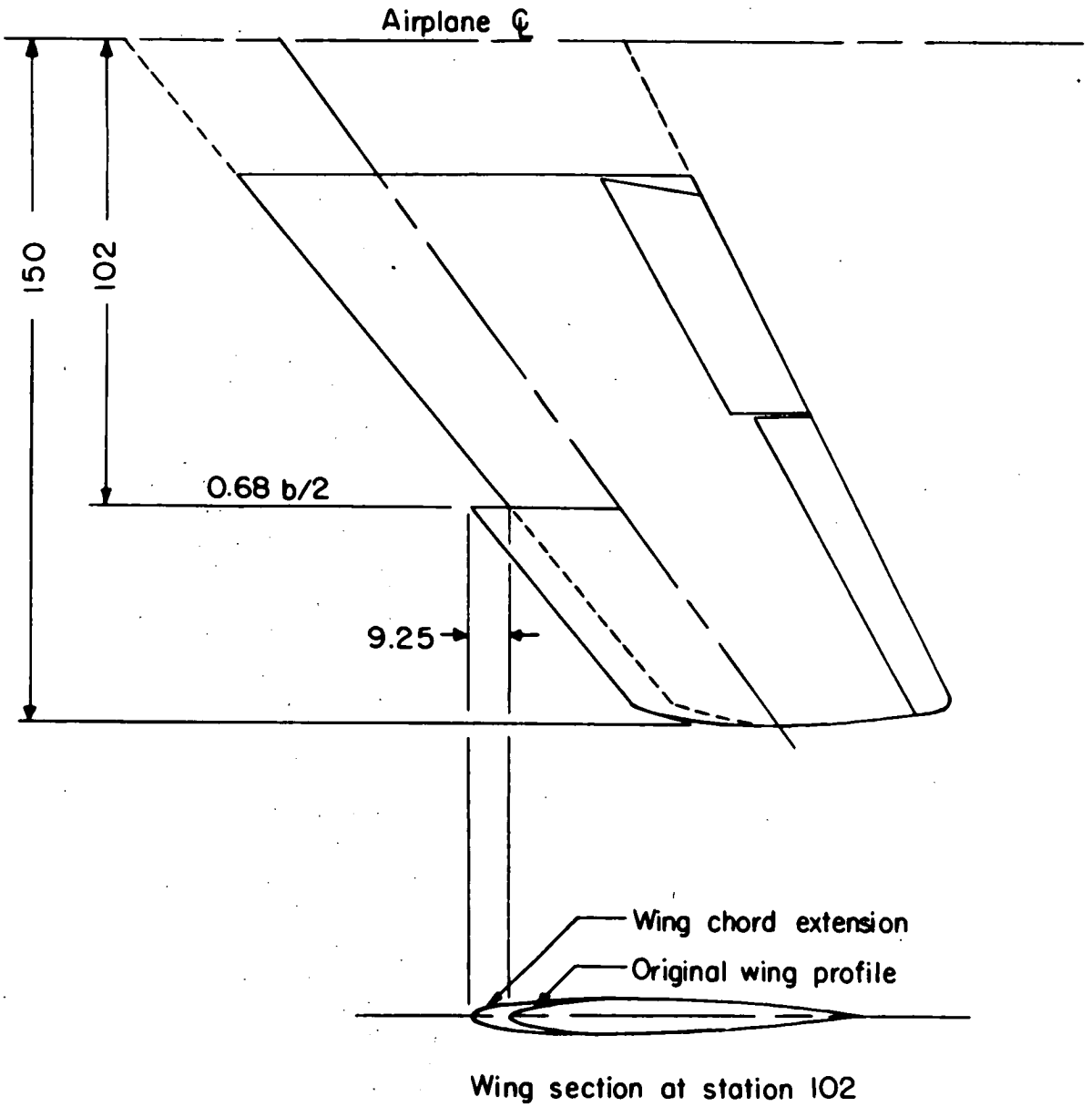

Figure 7.- Plan form and section of the wing of the D-558-II airplane showing the wing leading-edge chord-extension configuration.

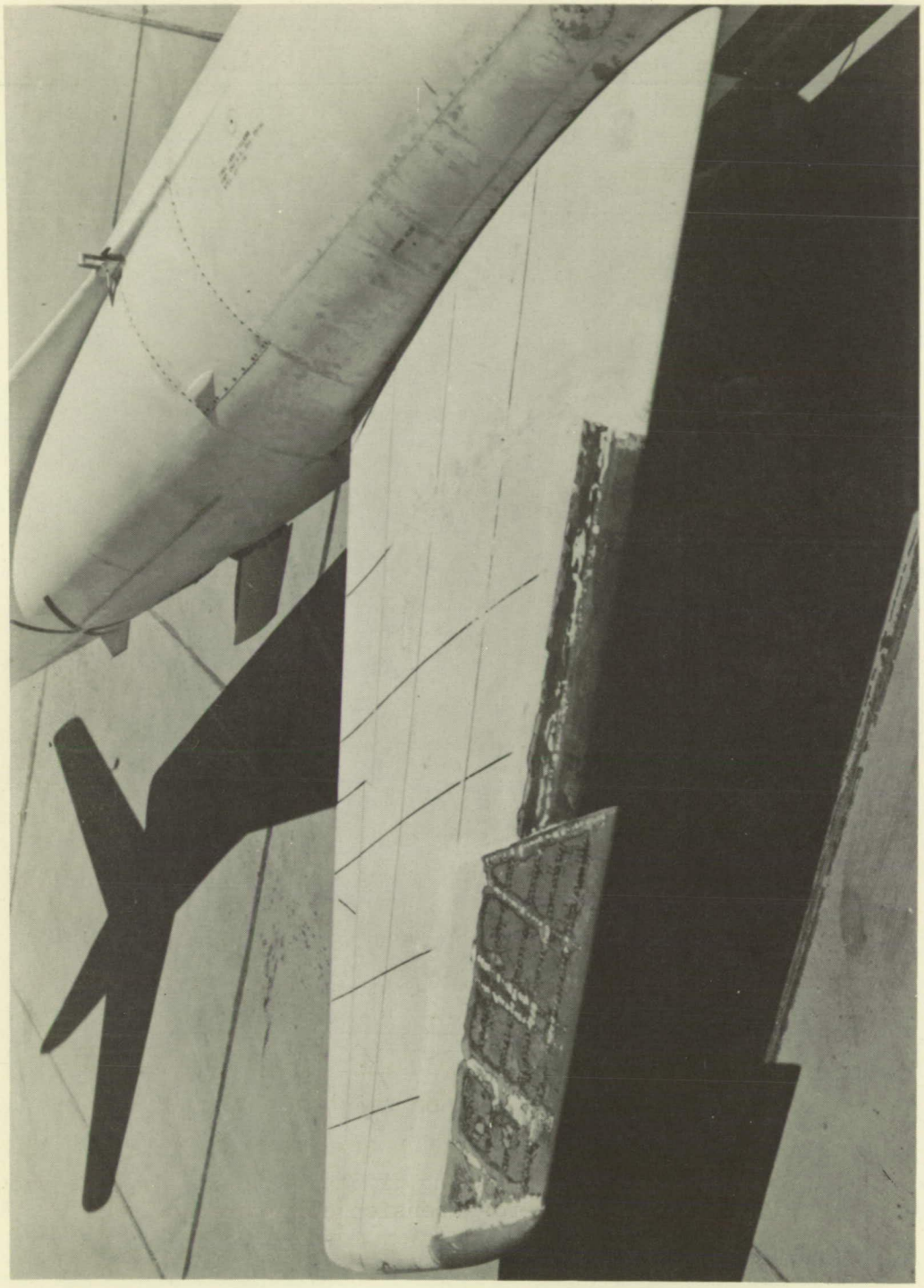

L-87976

Figure 8.- Photograph of the wing of the D-558-II airplane showing the wing leading-edge chord-extension configuration.

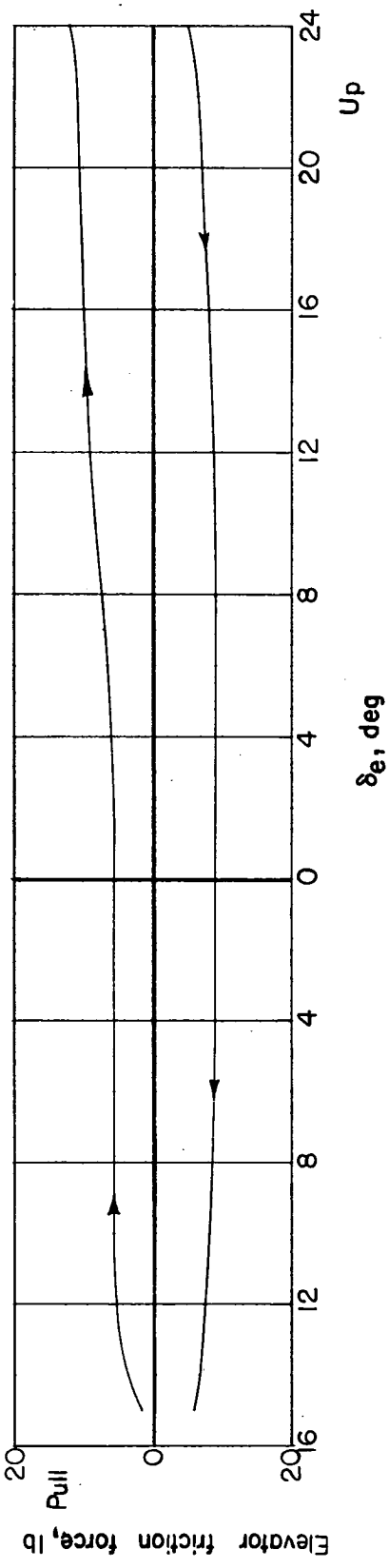

Figure 9.- Elevator-control force required to deflect elevator on the ground under no load.

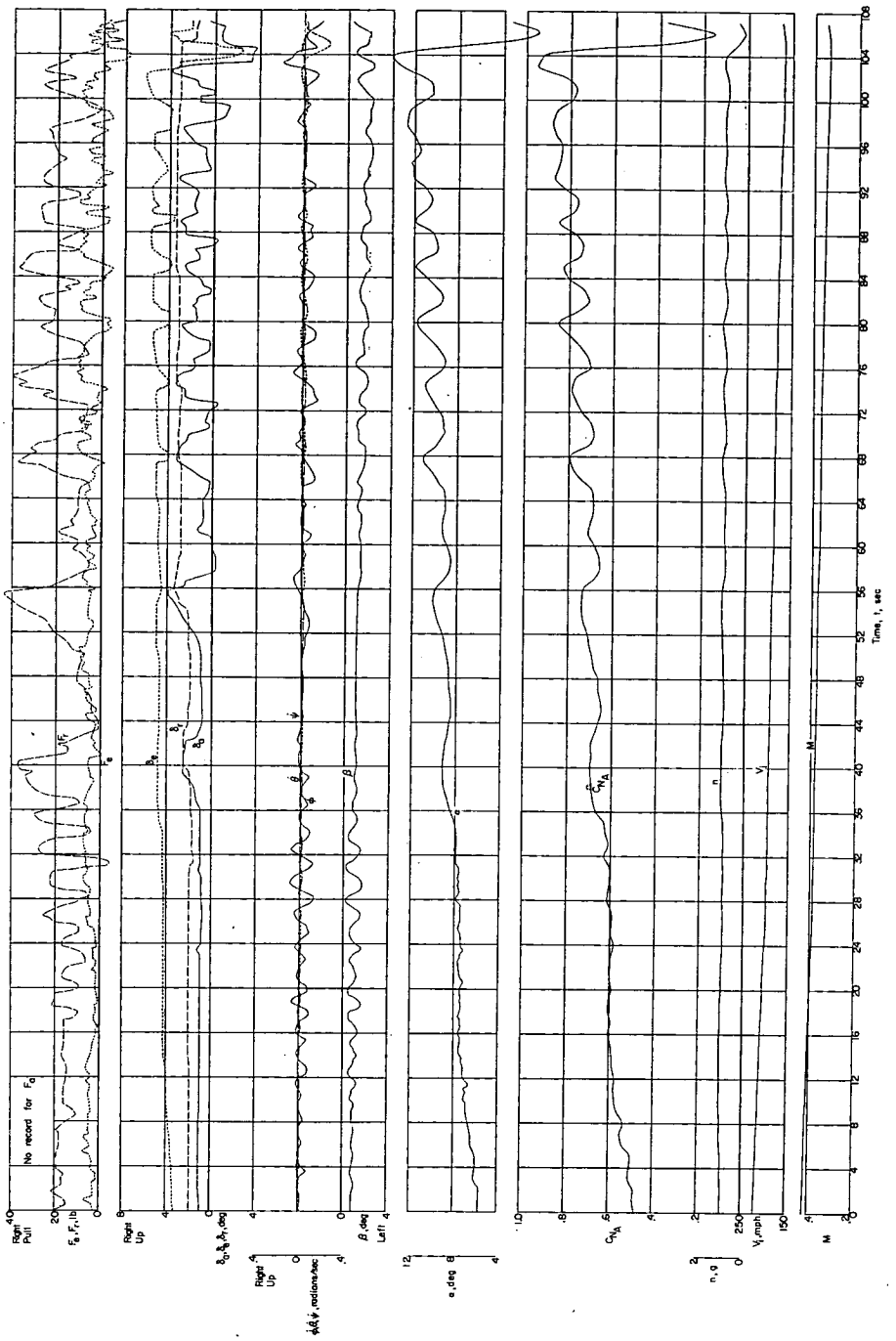

(a) Time history.

Figure 10.- Flight characteristics of the D-558-II research airplane during an unaccelerated stall. No fences on; slats retracted; flaps retracted; landing gear retracted; $i_t = 1.5°$; center of gravity at $0.26\bar{7}\bar{c}$; $h_p \approx 20{,}800$ feet.

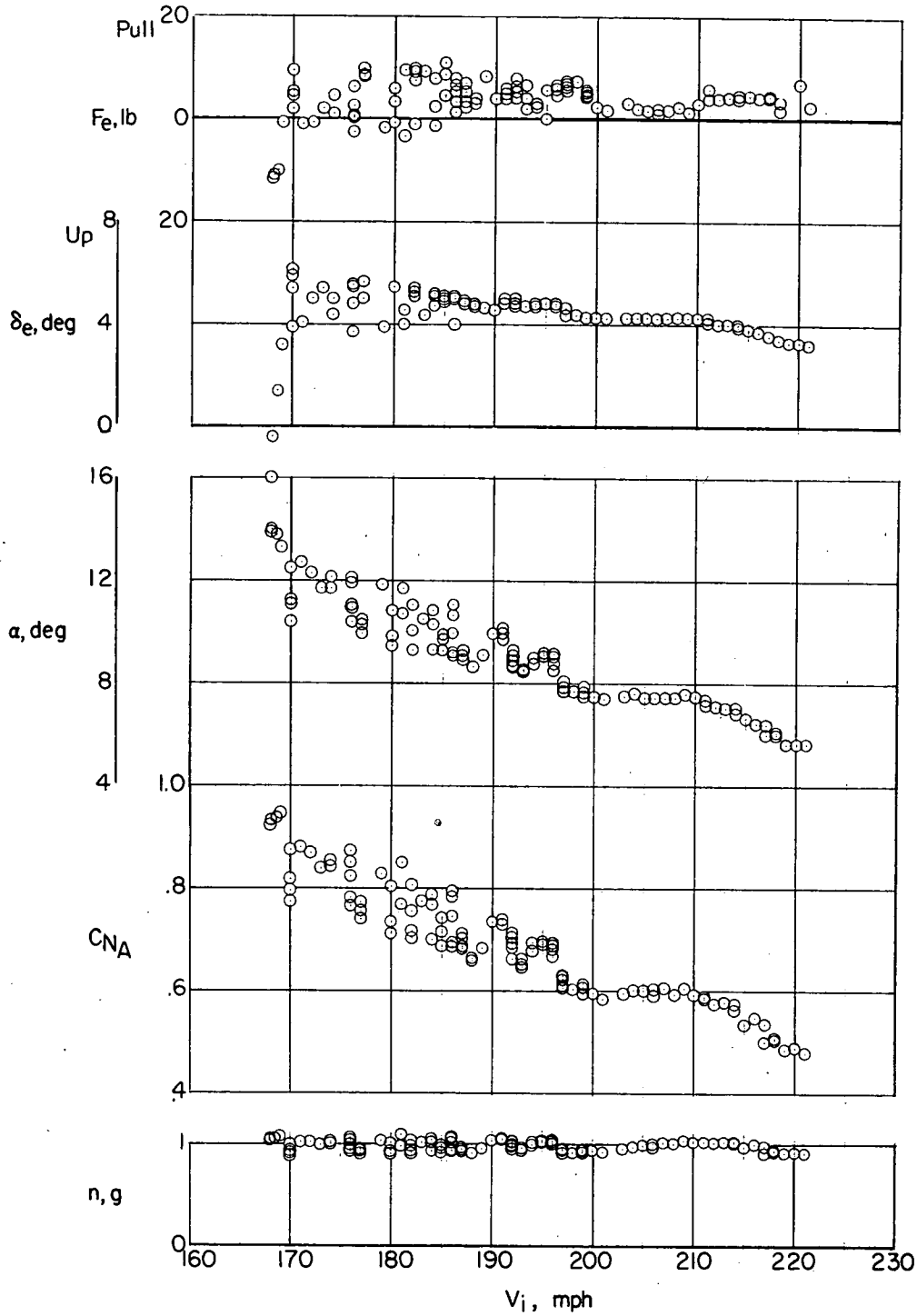

(b) Variation of F_e, δ_e, α, C_{N_A}, and n with V_i.

Figure 10.- Concluded.

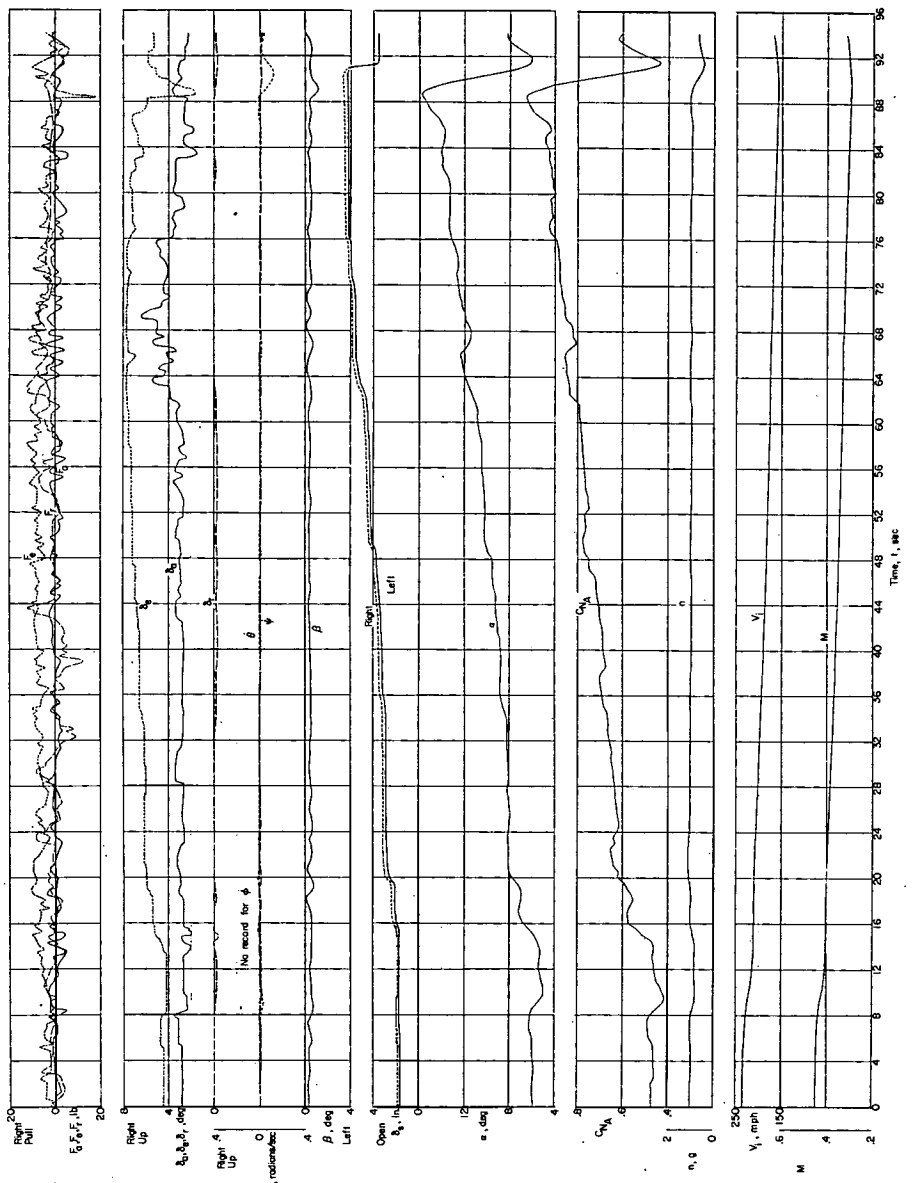

(a) Time history.

Figure 11.- Flight charateristics of the D-558-II research airplane during an unaccelerated stall. No fences on; slats unlocked; flaps retracted; landing gear retracted; $i_t = 1.5°$; center of gravity at 0.26$\bar{c}$; $h_p \approx 19{,}500$ feet.

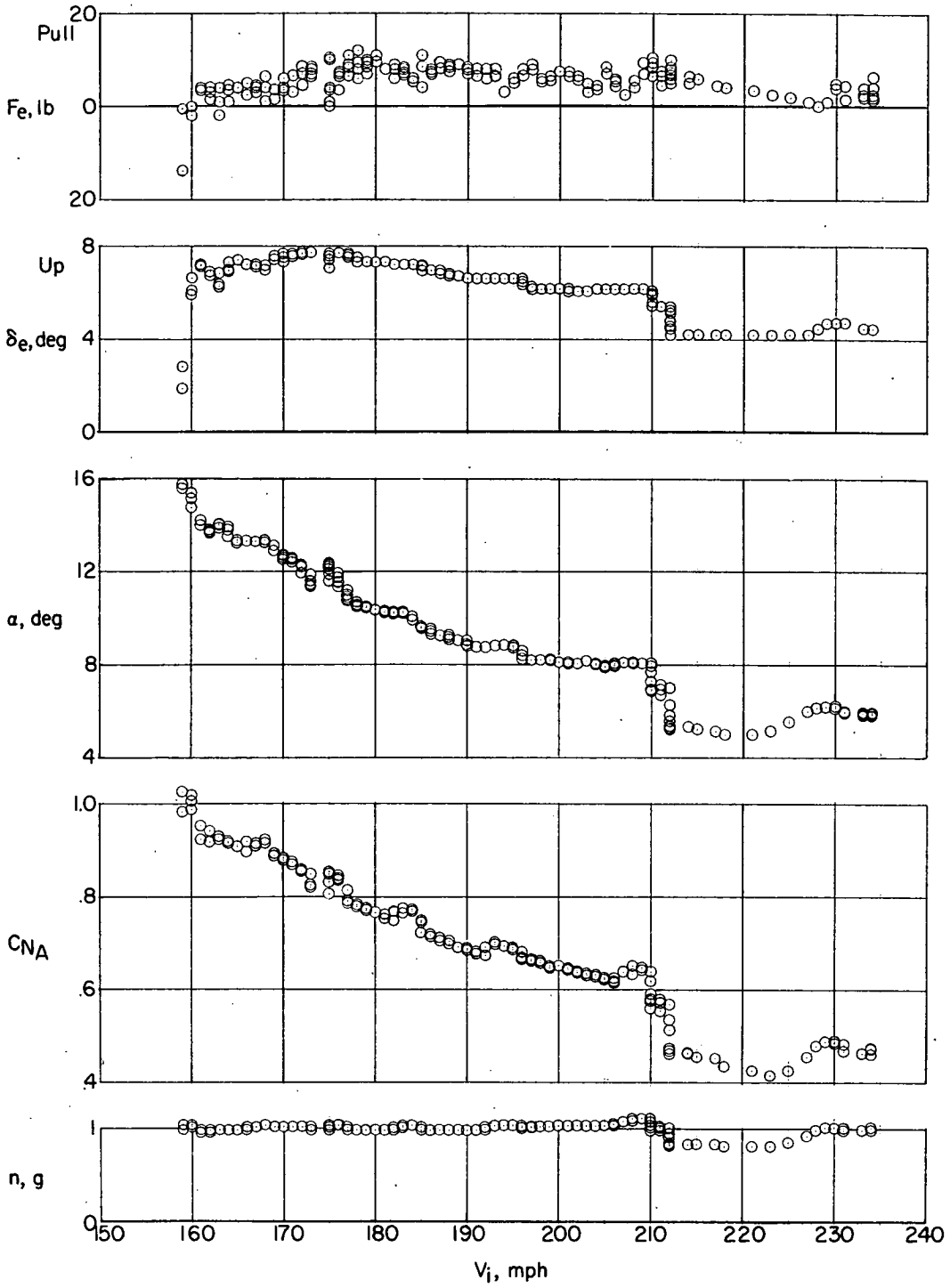

(b) Variation of F_e, δ_e, α, C_{N_A}, and n with V_i.

Figure 11.- Concluded.

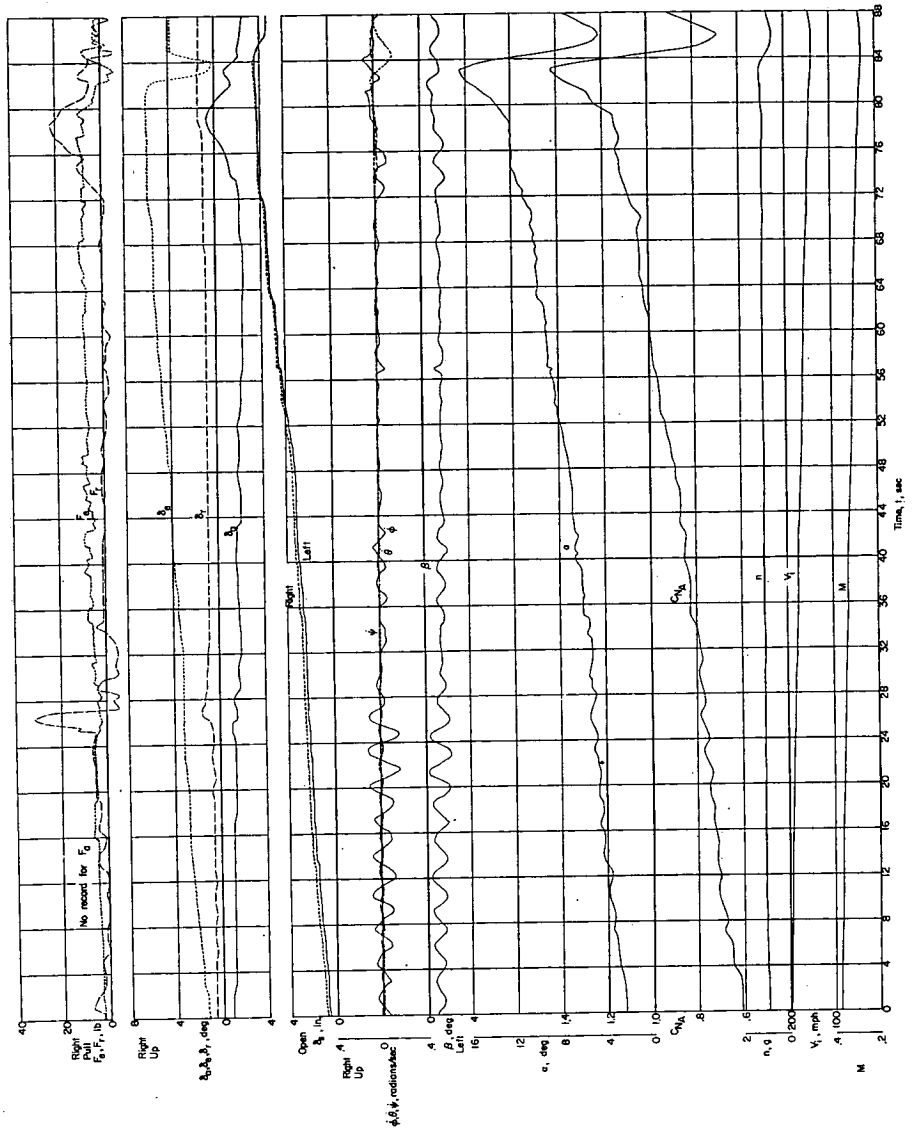

(a) Time history.

Figure 12.- Flight characteristics of the D-558-II research airplane during an unaccelerated stall. No fences on; slats unlocked; flaps extended; landing gear extended; $i_t = 1.5°$; center of gravity at $0.260\bar{c}$; $h_p \approx 19{,}000$ feet.

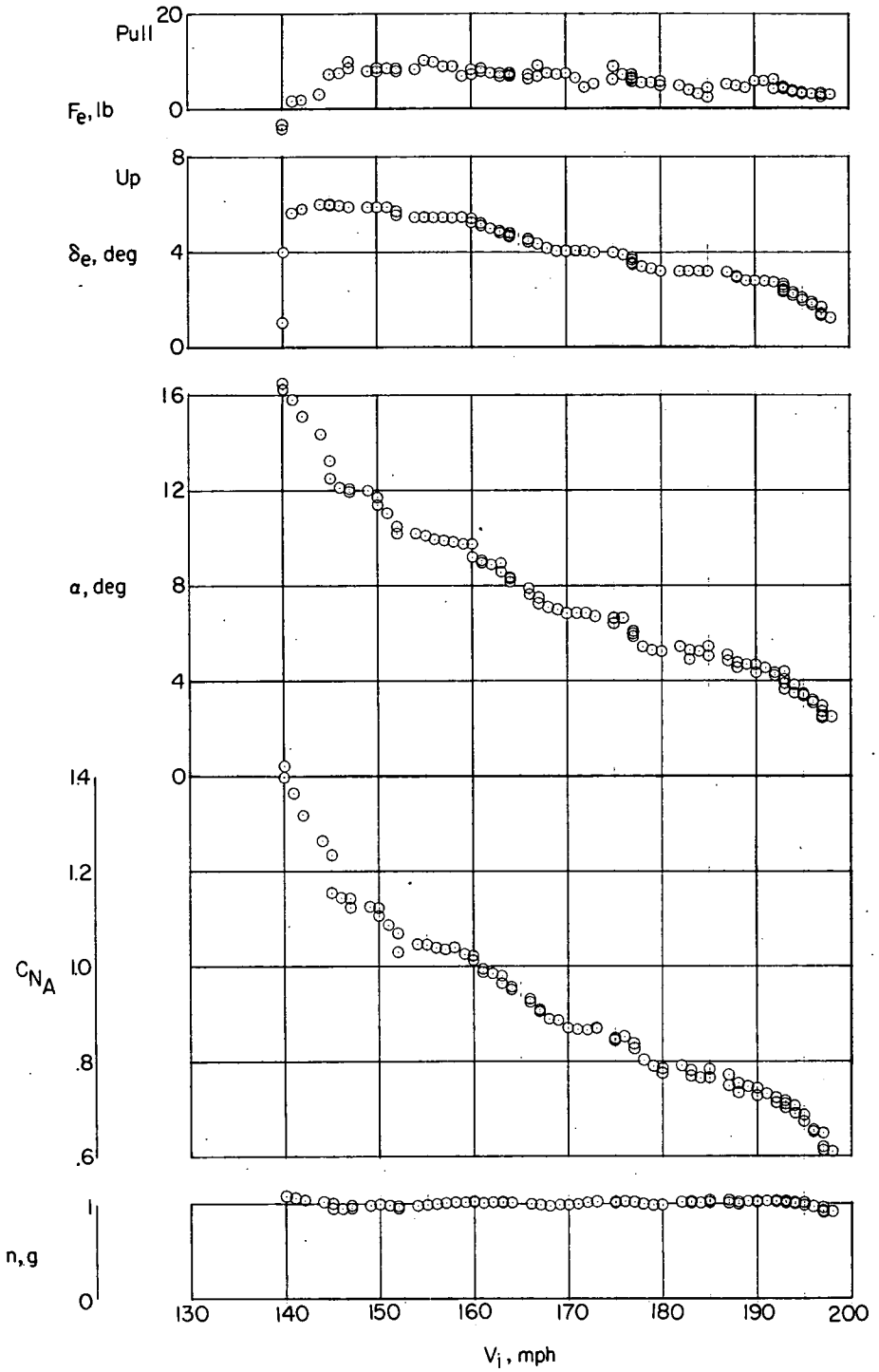

(b) Variation of F_e, δ_e, α, C_{N_A}, and n with V_i.

Figure 12.- Concluded.

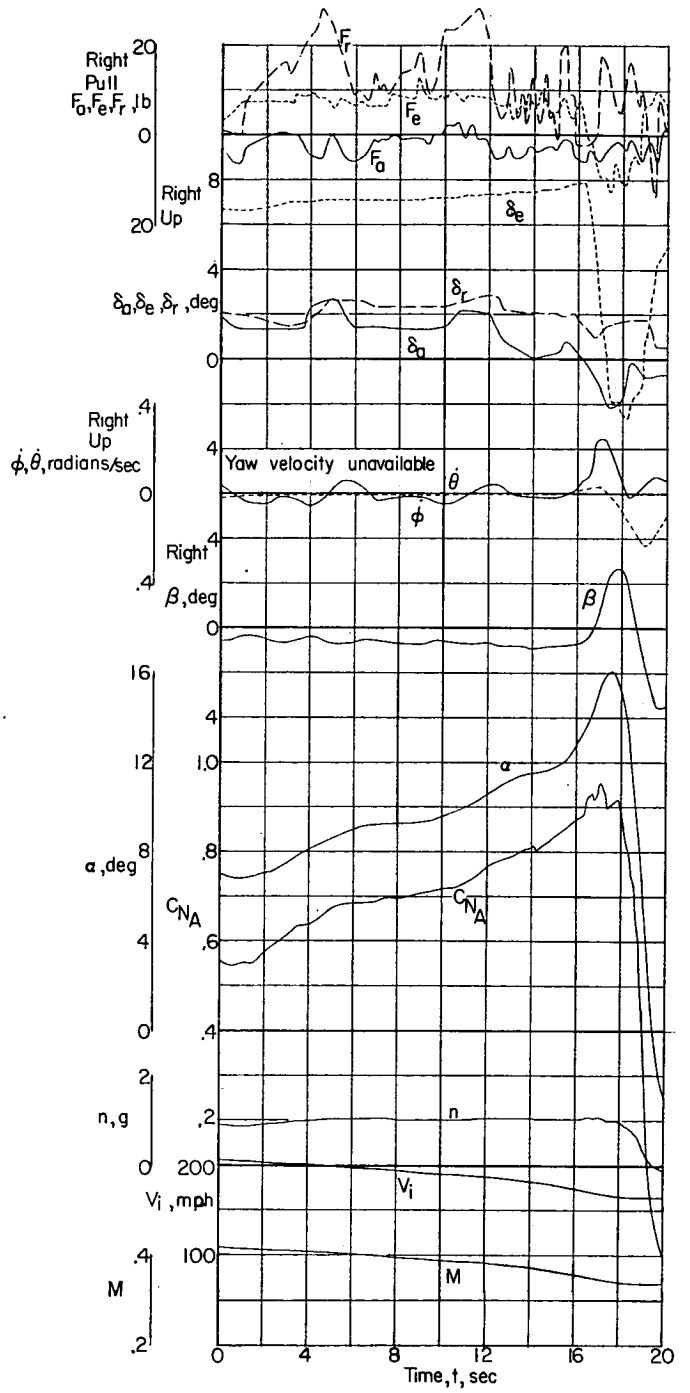

(a) Time history.

Figure 13.- Flight characteristics of the D-558-II research airplane during an unaccelerated stall. Inboard fences on; slats retracted; flaps retracted; landing gear retracted; $i_t = 1.3°$; center of gravity at $0.264\bar{c}$; $h_p \approx 20{,}000$ feet.

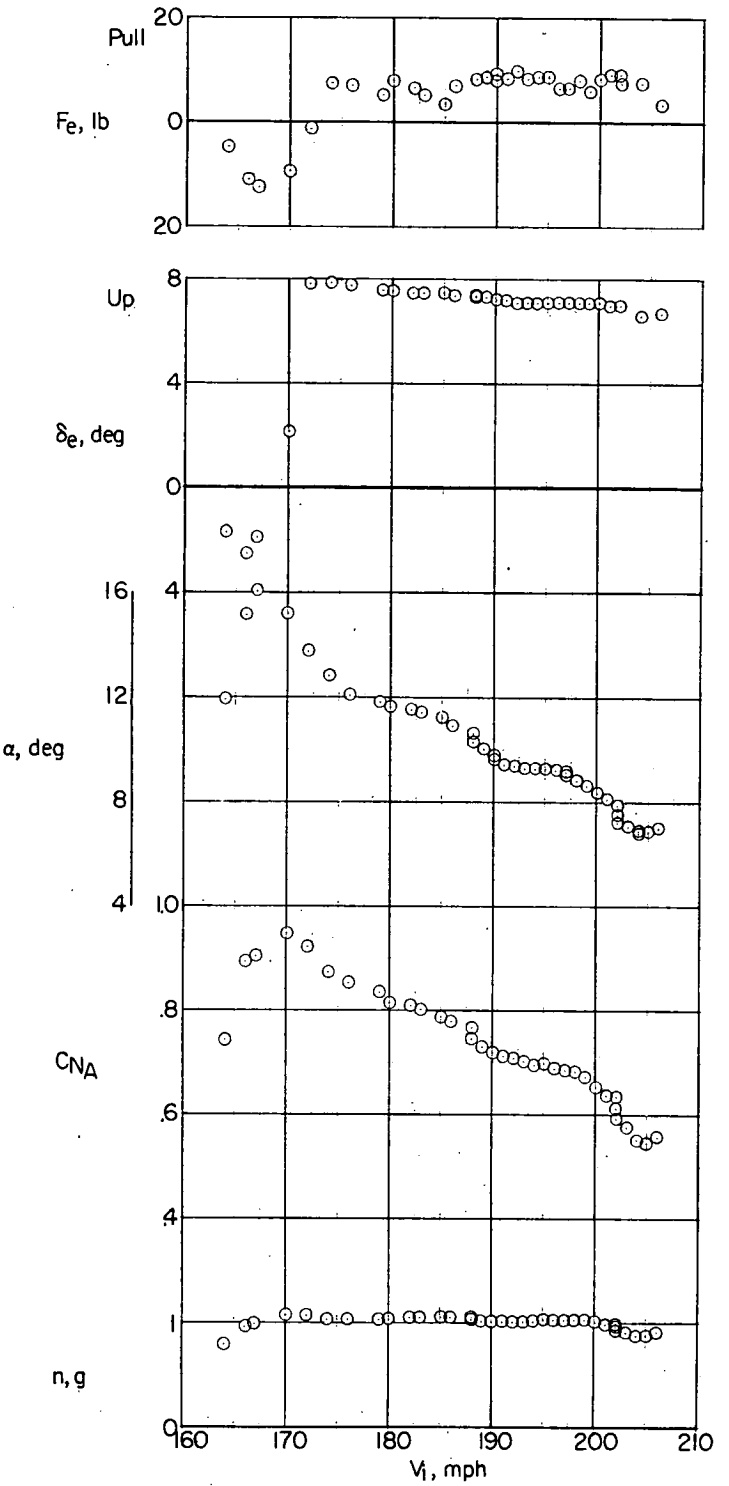

(b) Variation of F_e, δ_e, α, C_{N_A}, and n with V_i.

Figure 13.- Concluded.

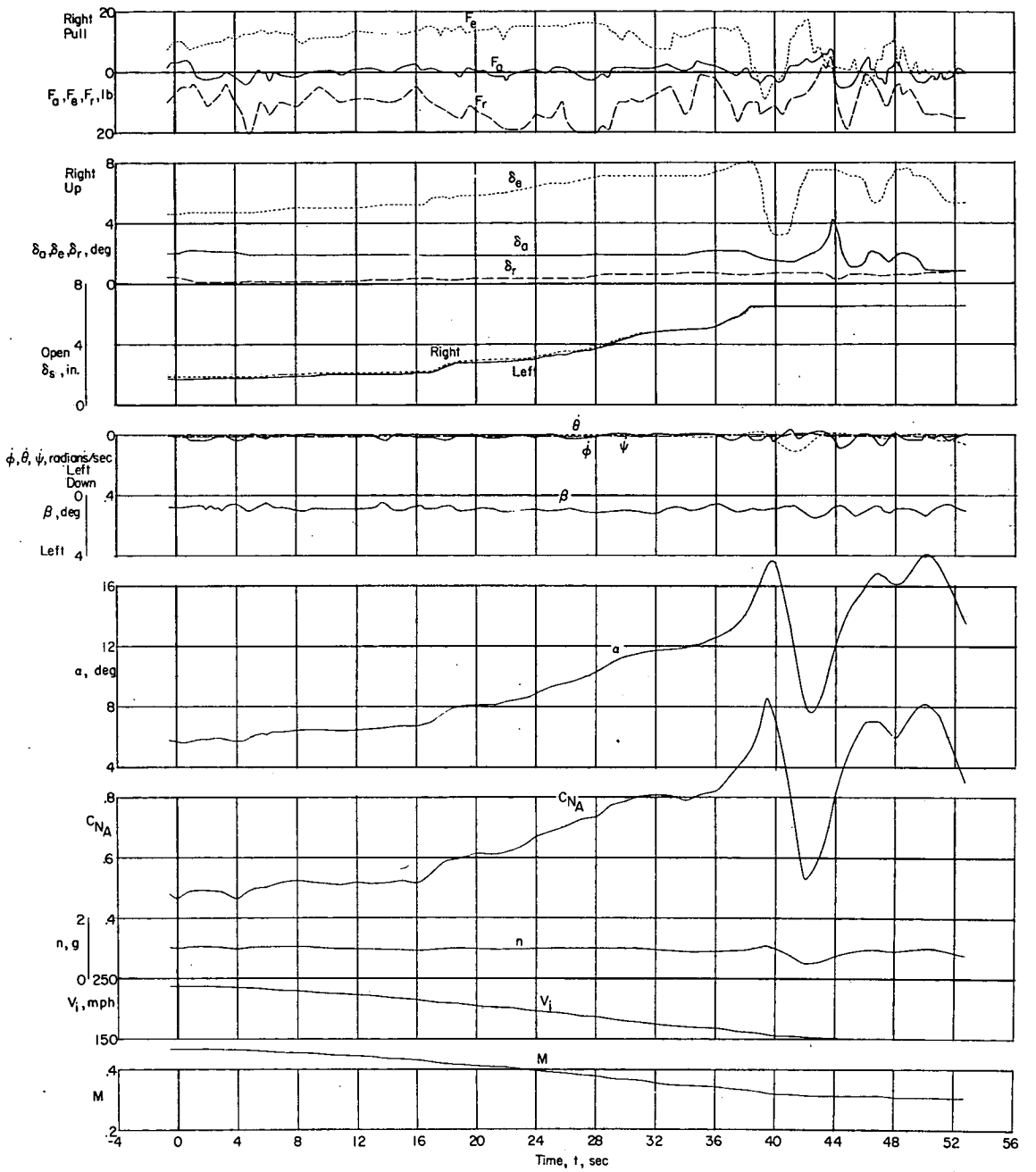

(a) Time history.

Figure 14.- Flight characteristics of the D-558-II research airplane during an unaccelerated stall. Inboard fences on; slats unlocked; flaps retracted; landing gear retracted; $i_t = 2.1^\circ$; center of gravity at $0.255\bar{c}$; $h_p \approx 21{,}000$ feet.

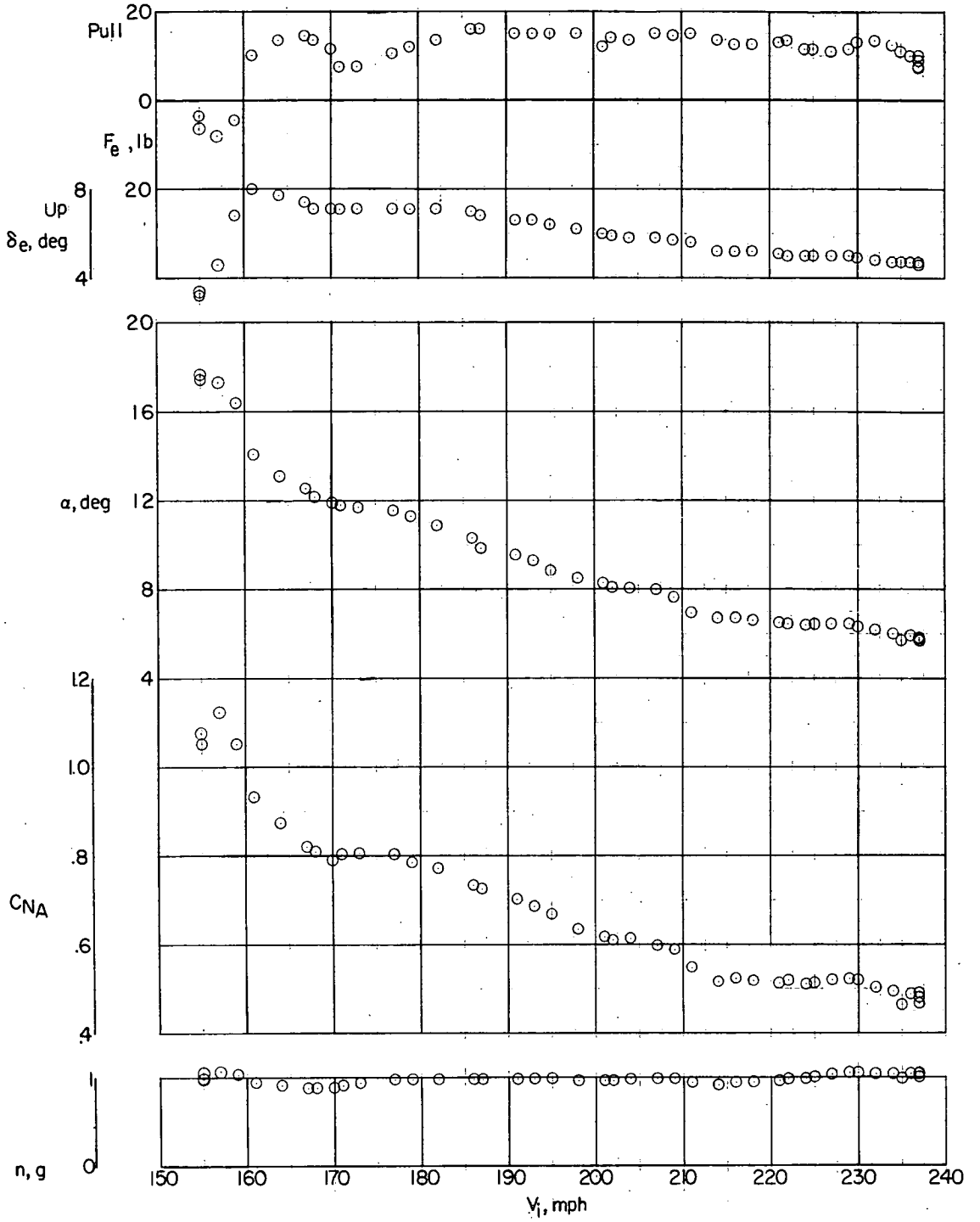

(b) Variation of F_e, δ_e, α, C_{N_A}, and n with V_i.

Figure 14.- Concluded.

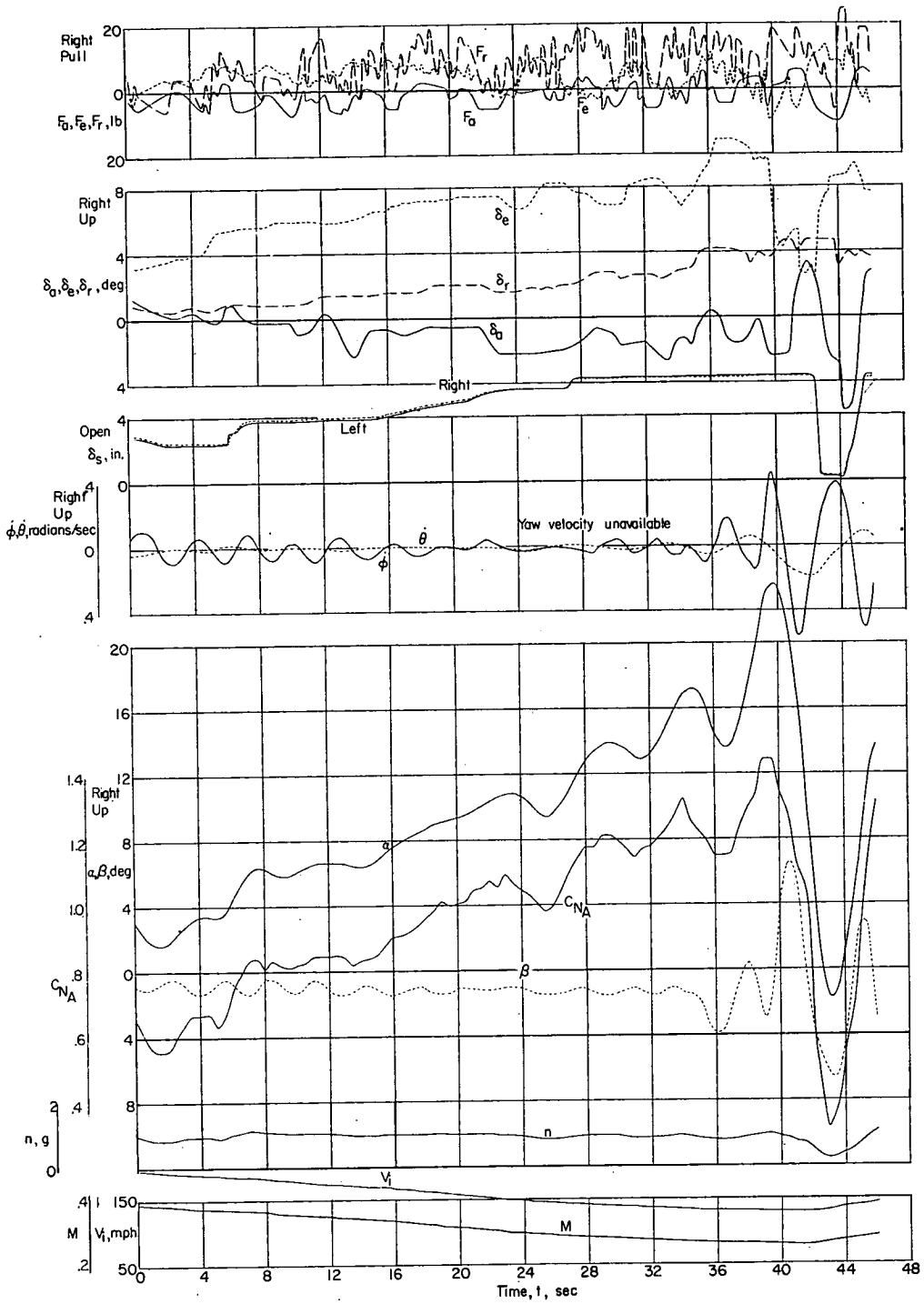

(a) Time history.

Figure 15.- Flight characteristics of the D-558-II research airplane during an unaccelerated stall. Inboard fences on; slats unlocked; flaps extended; landing gear extended; $i_t = 1.4^\circ$; center of gravity at $0.253\bar{c}$; $h_p \approx 21{,}500$ feet.

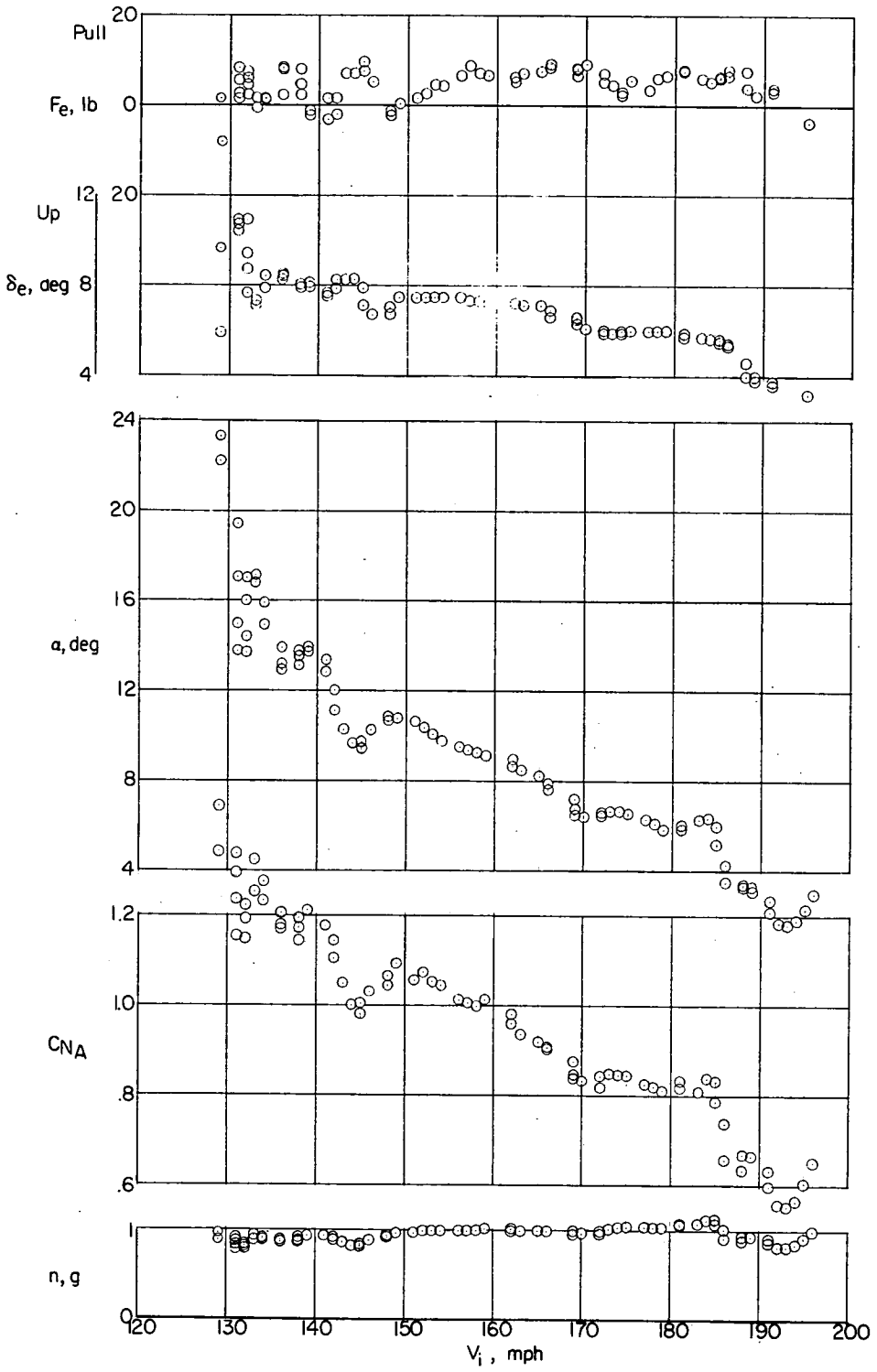

(b) Variation of F_e, δ_e, α, C_{N_A}, and n with V_i.

Figure 15.- Concluded.

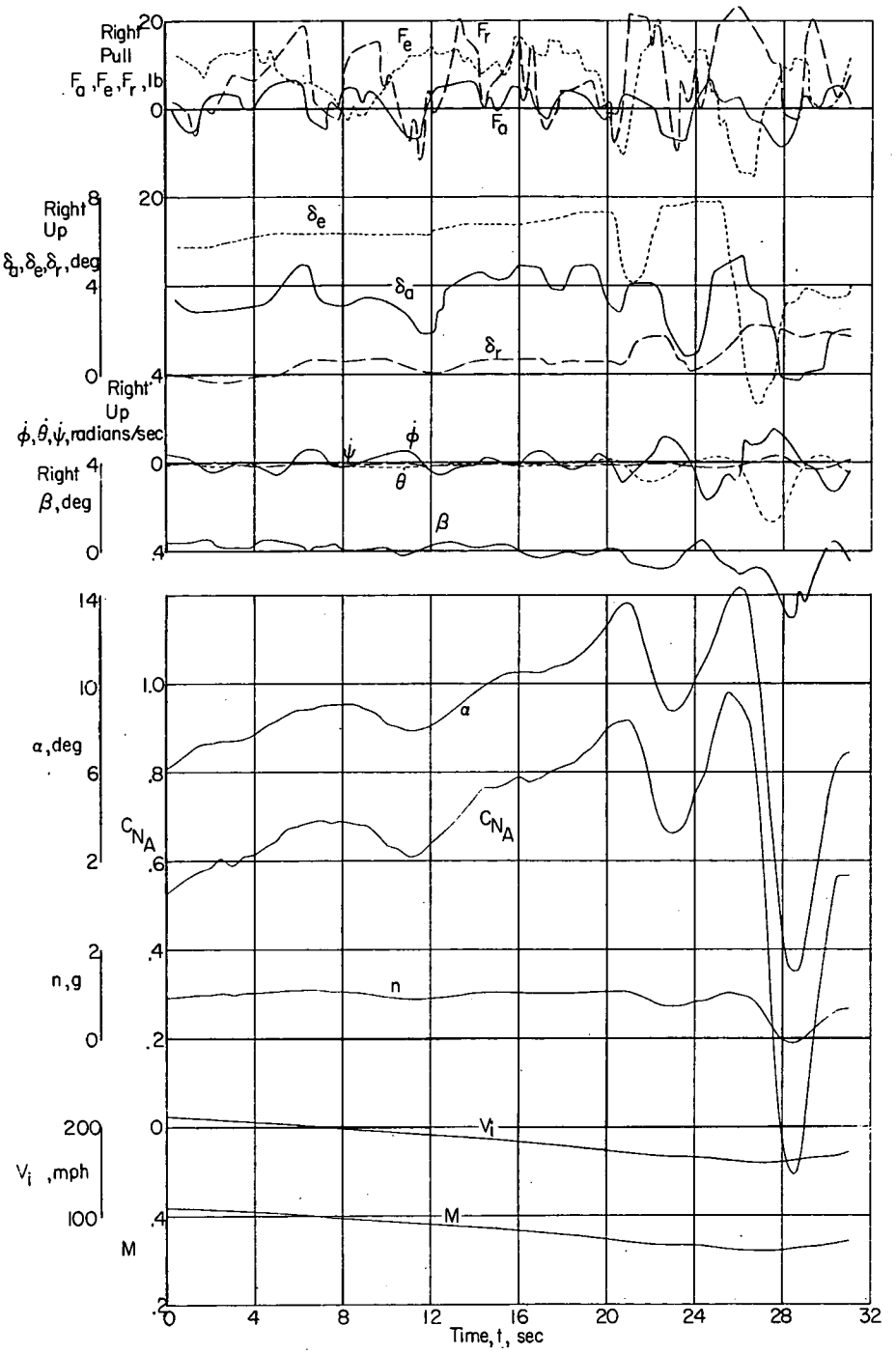

(a) Time history.

Figure 16.- Flight characteristics of the D-558-II research airplane during an unaccelerated stall. Both fences on; slats retracted; flaps retracted; landing gear retracted; $i_t = 2.3^\circ$; center of gravity at $0.262\bar{c}$; $h_p \approx 21{,}000$ feet.

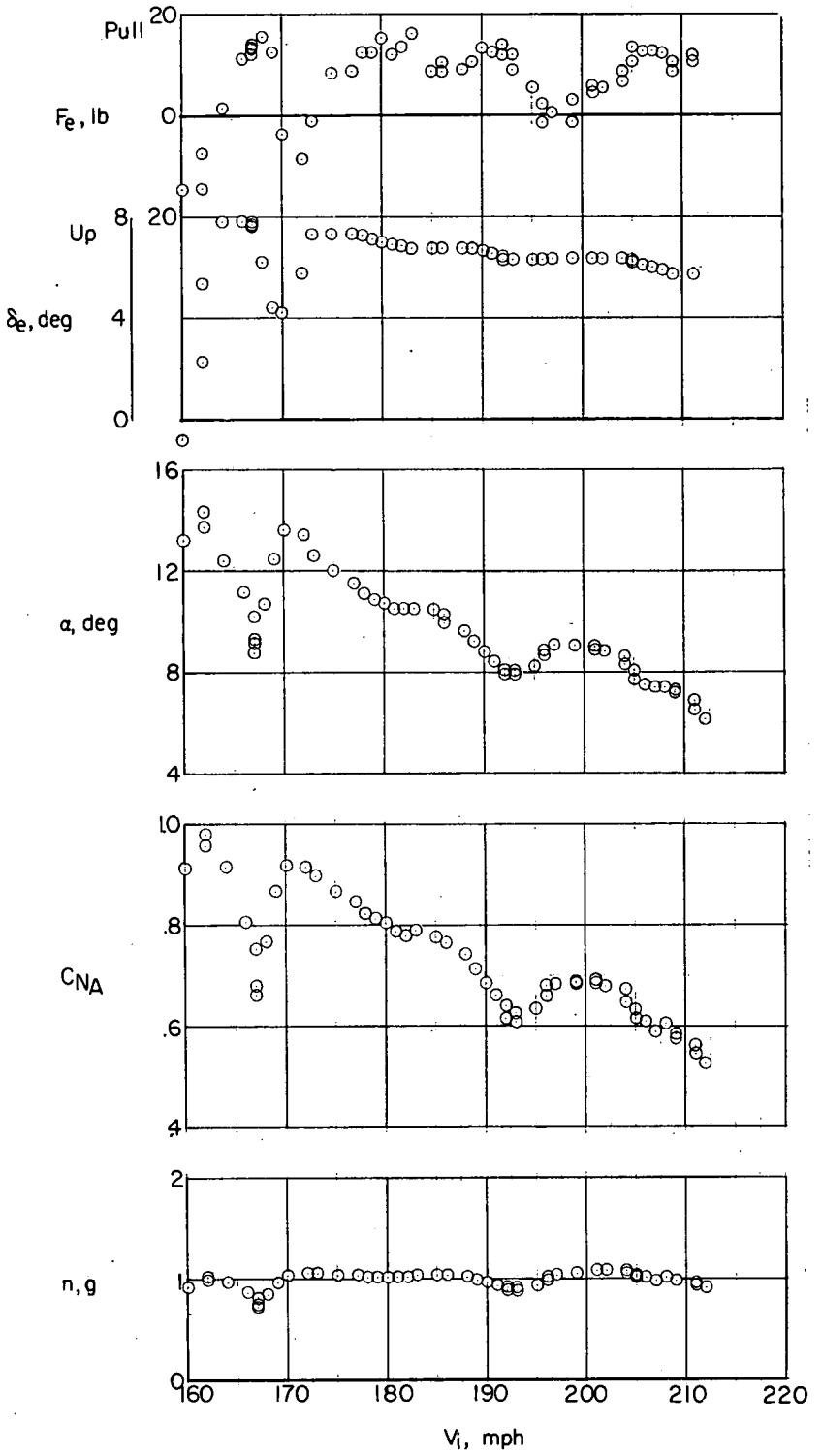

(b) Variation of F_e, δ_e, α, C_{N_A}, and n with V_i.

Figure 16.- Concluded.

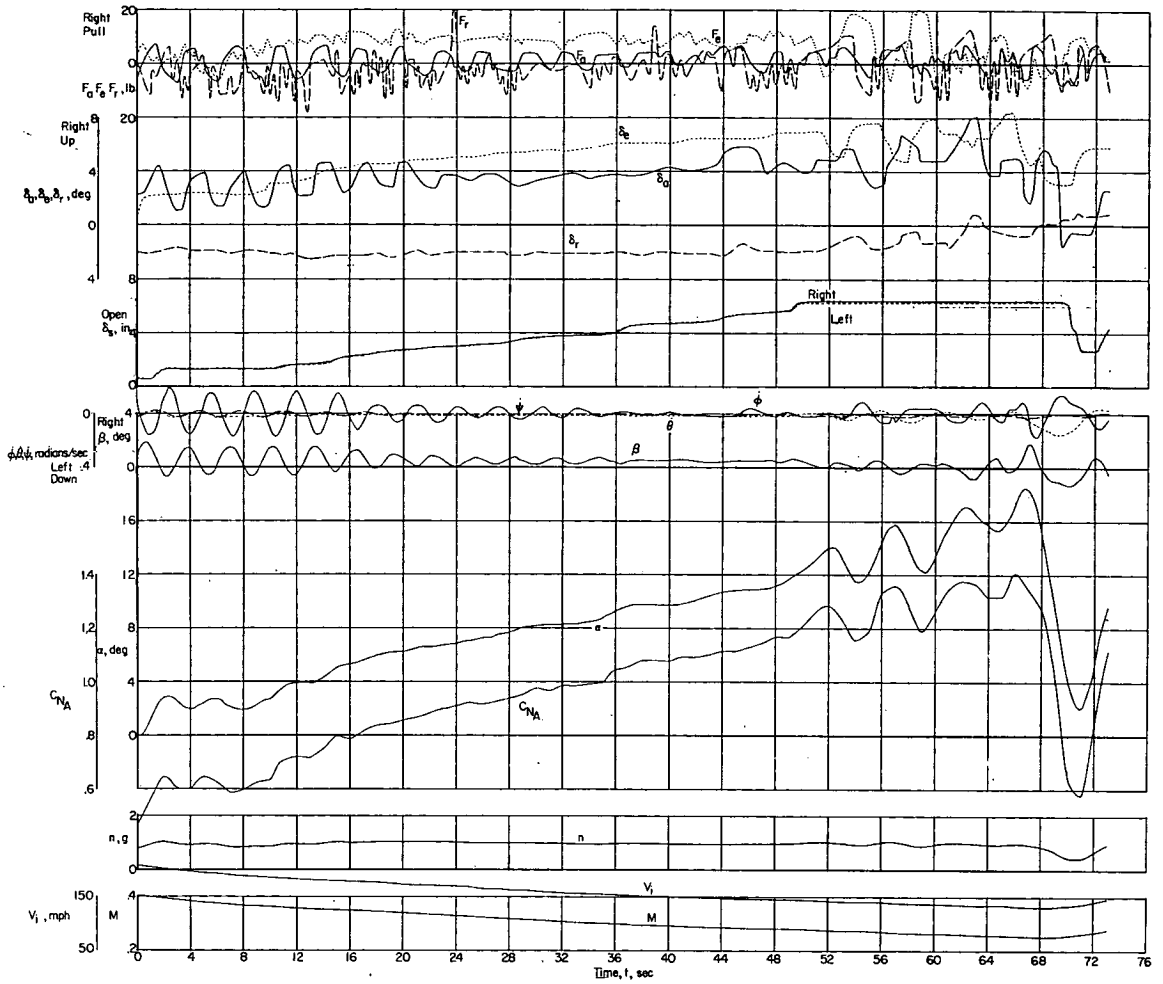

(a) Time history.

Figure 17.- Flight characteristics of the D-558-II research airplane during an unaccelerated stall. Inboard and outboard wing fences installed; slats unlocked; flaps extended; landing gear extended; $i_t = 2.3^\circ$; center of gravity at $0.262\bar{c}$; $h_p \approx 20{,}500$ feet.

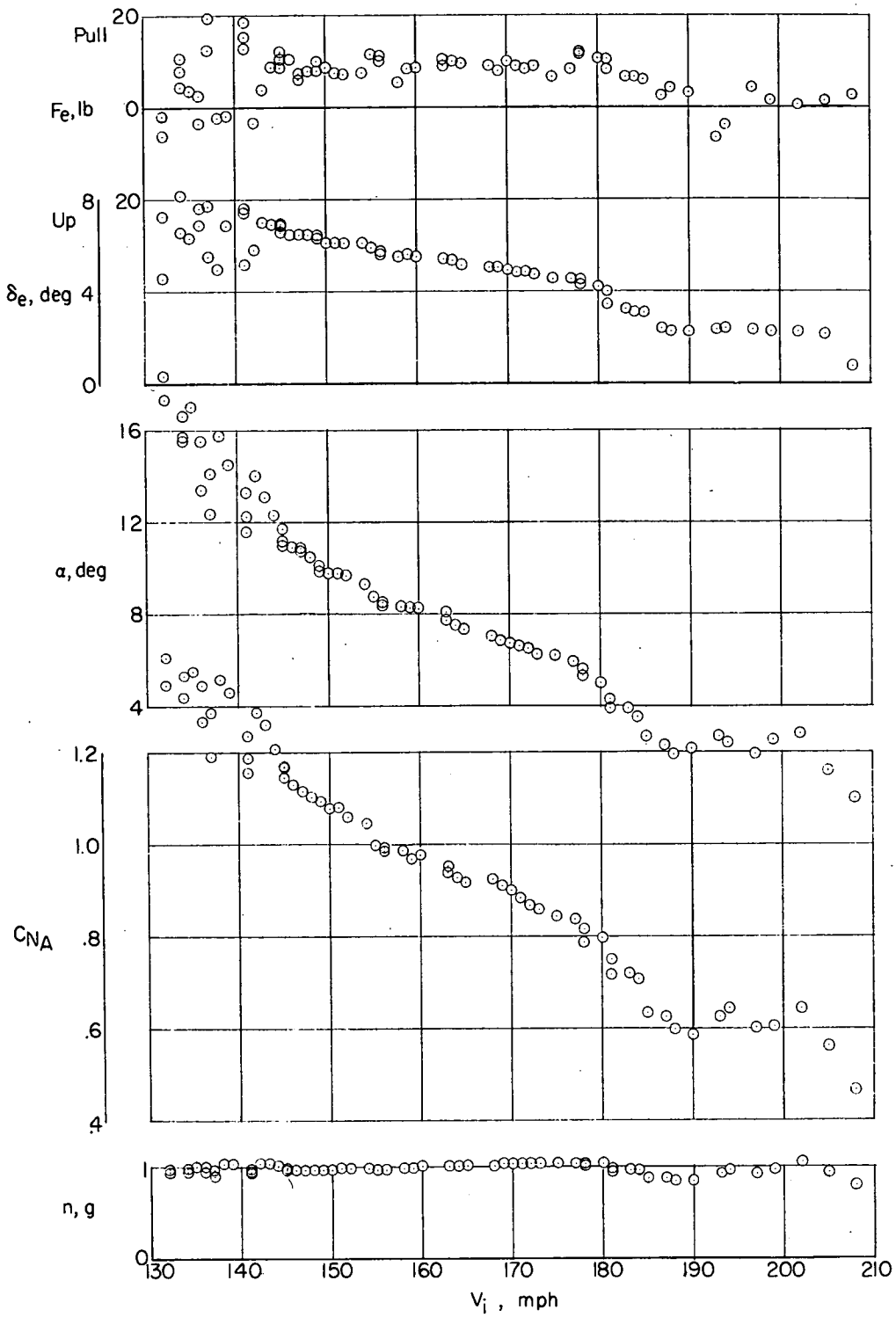

(b) Variation of F_e, δ_e, α, C_{N_A}, and n with V_i.

Figure 17.- Concluded.

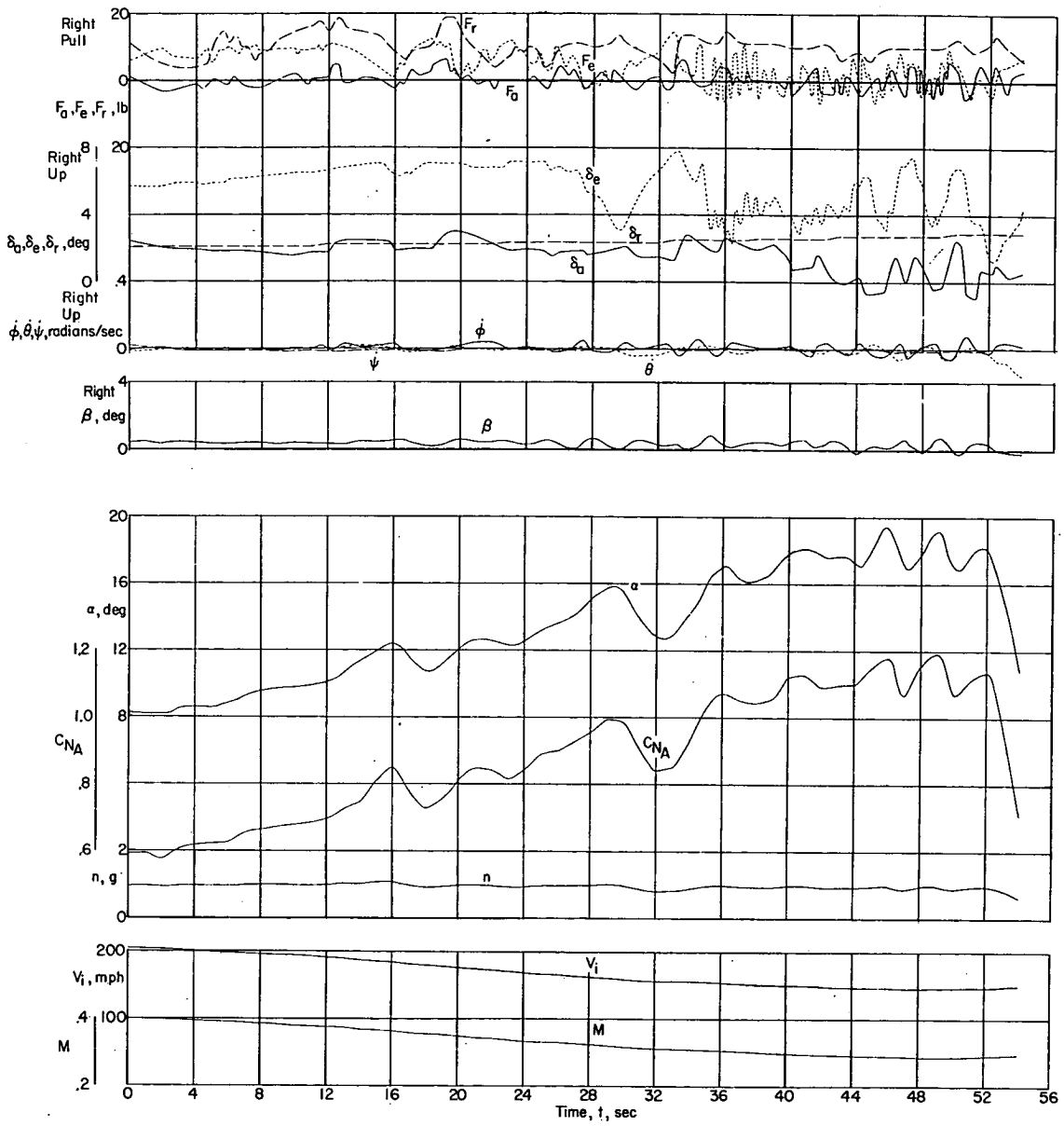

(a) Time history.

Figure 18.- Flight characteristics of the D-558-II research airplane during an unaccelerated stall. No fences on; slats fully extended; flaps retracted; landing gear retracted; $i_t = 1.6^\circ$; center of gravity at $0.253\bar{c}$; $h_p \approx 21{,}000$ feet.

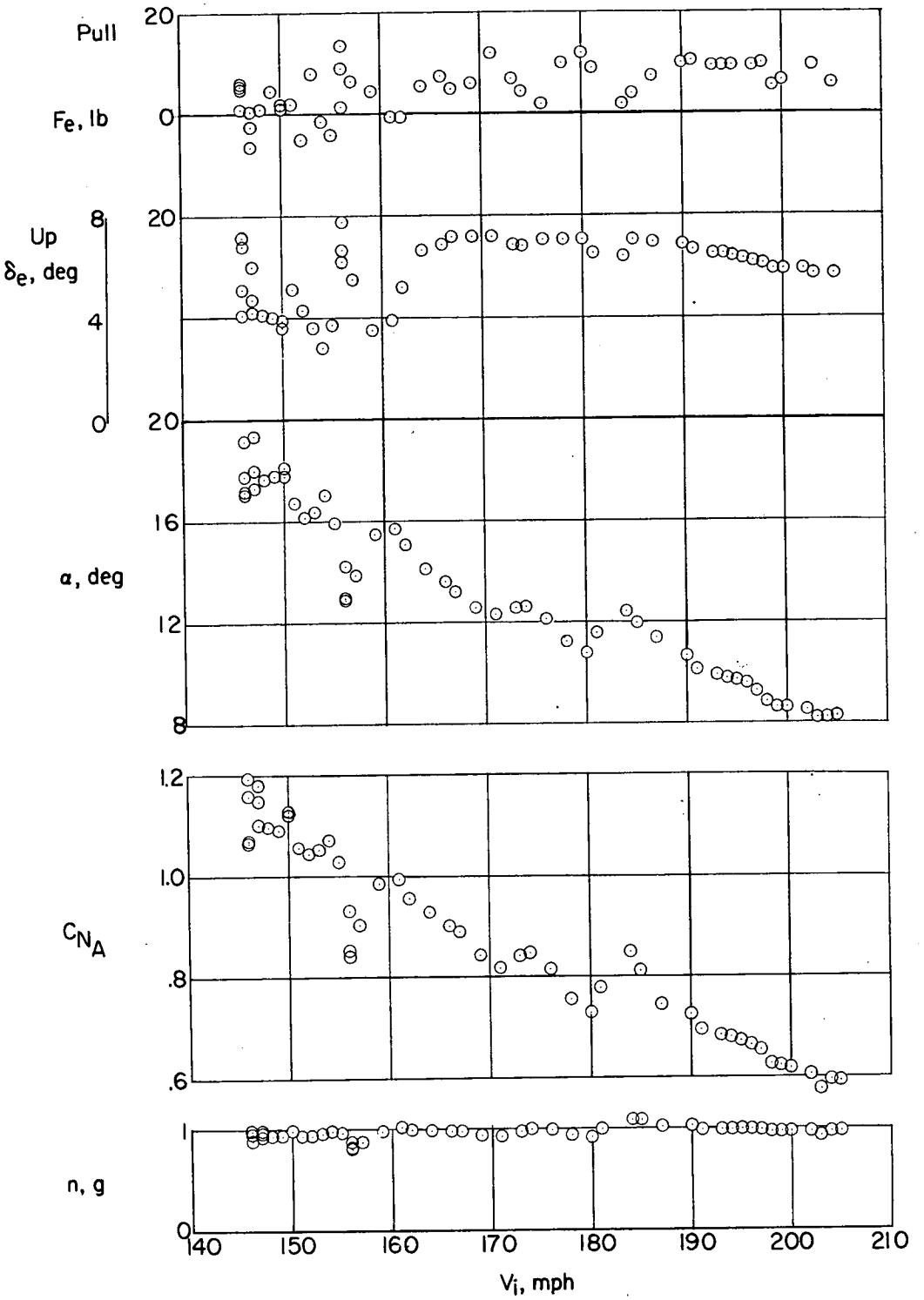

(b) Variation of F_e, δ_e, α, C_{N_A}, and n with V_i.

Figure 18.- Concluded.

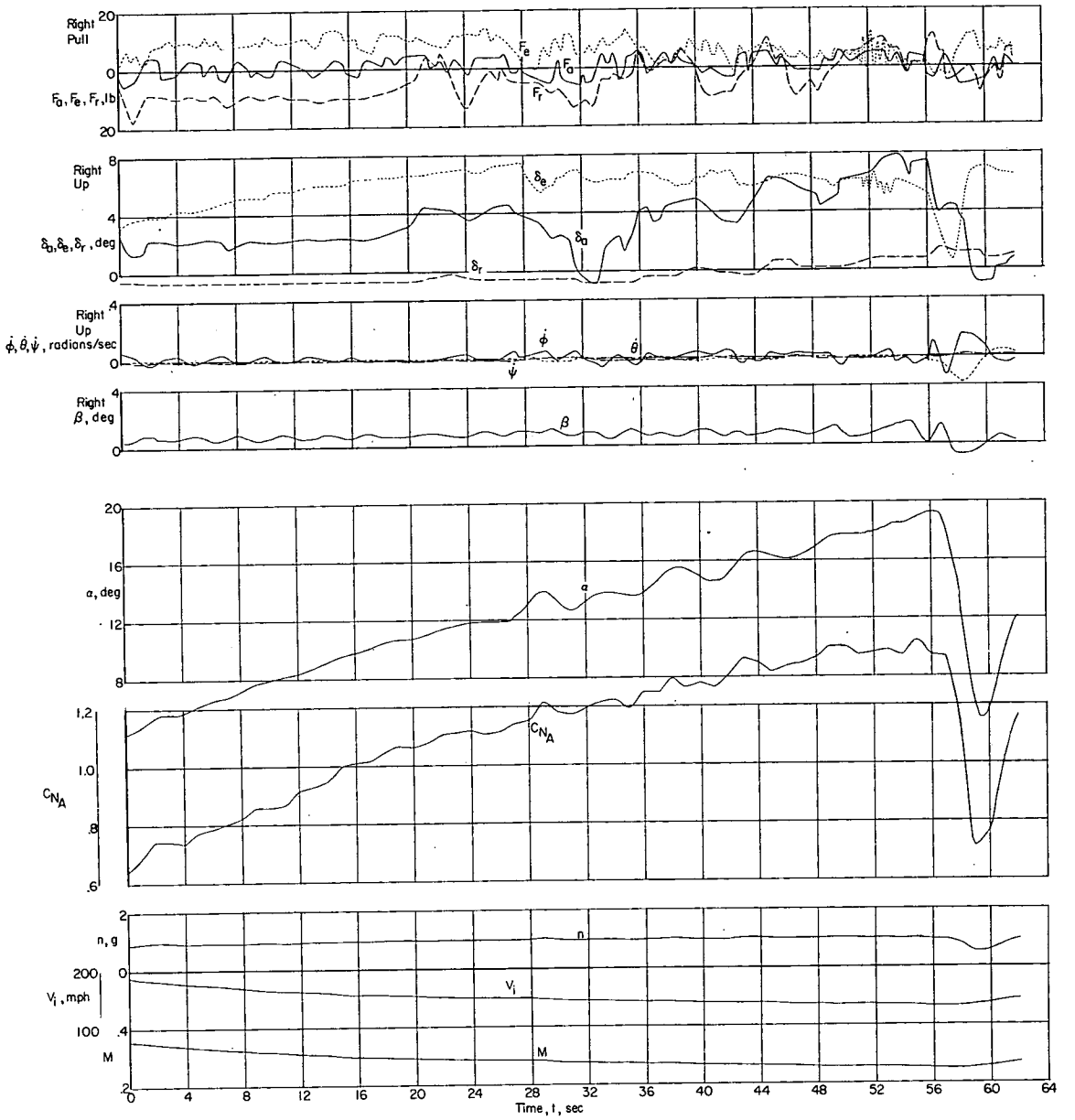

(a) Time history.

Figure 19.- Flight characteristics of the D-558-II research airplane during an unaccelerated stall. No fences on; slats fully extended; flaps extended; landing gear extended; $i_t = 1.6^\circ$; center of gravity at $0.249\bar{c}$; $h_p \approx 19{,}000$ feet.

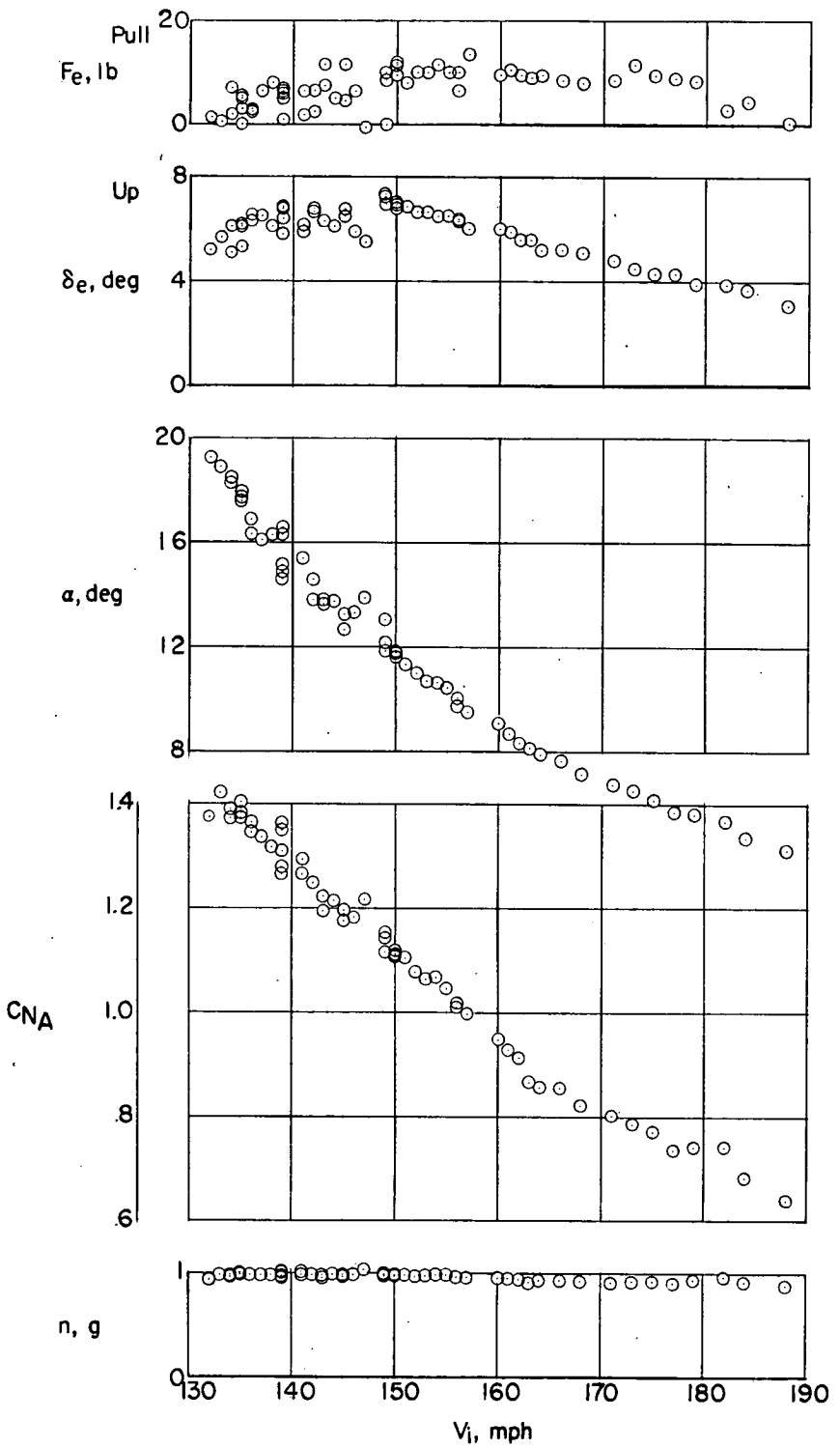

(b) Variation of F_e, δ_e, α, C_{N_A}, and n with V_i.

Figure 19.- Concluded.

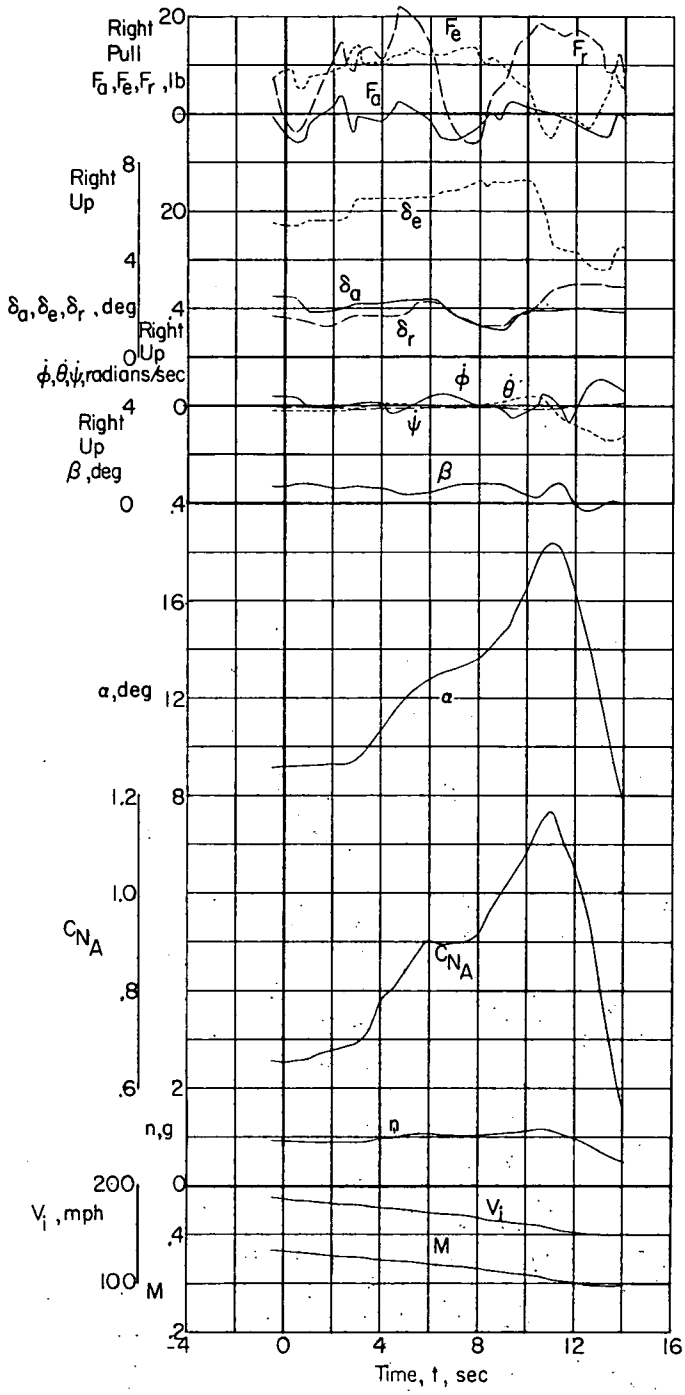

(a) Time history.

Figure 20.- Flight characteristics of the D-558-II research airplane during an unaccelerated stall. Inboard fences on; slats fully extended; flaps retracted; landing gear retracted; $i_t = 1.6^\circ$; center of gravity at $0.256\bar{c}$; $h_p \approx 21{,}000$ feet.

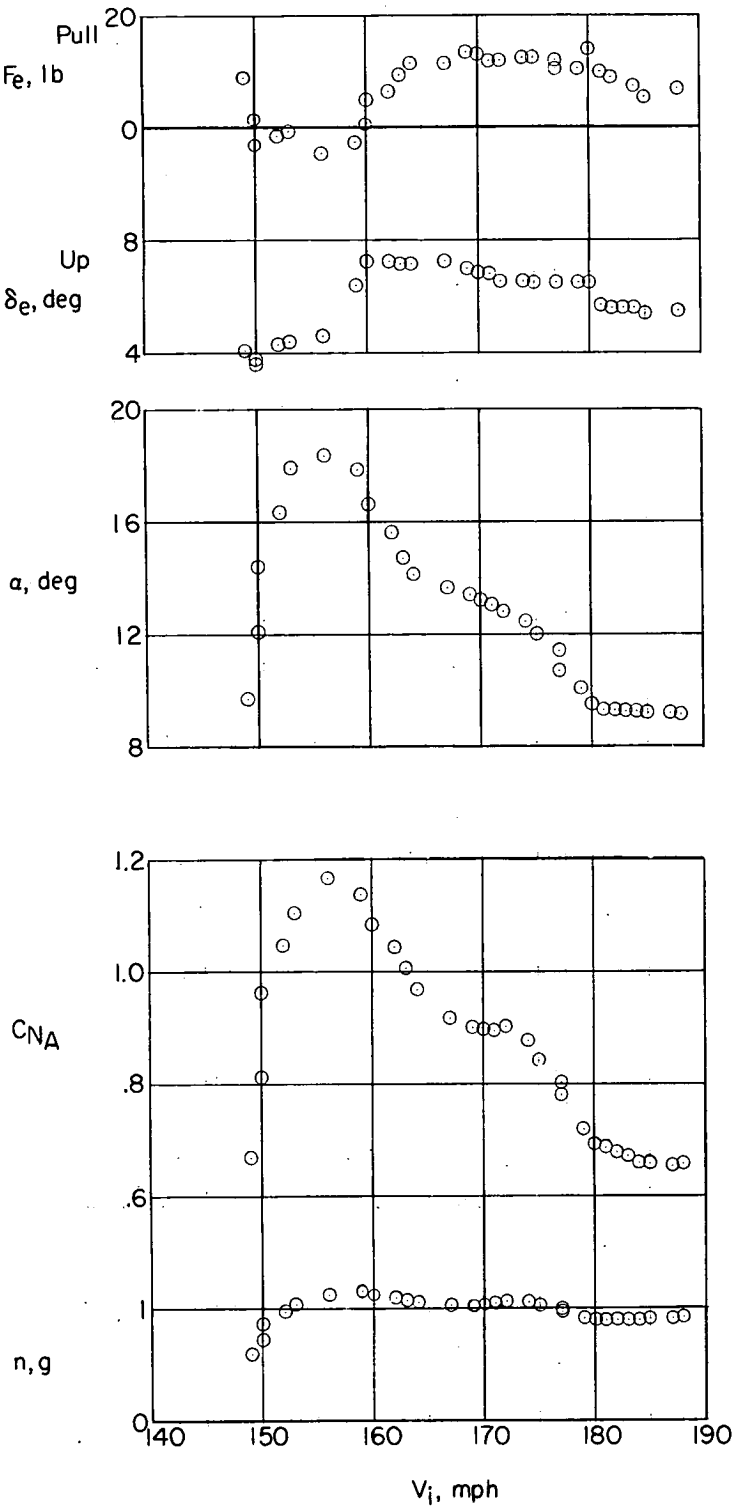

(b) Variation of F_e, δ_e, α, C_{N_A}, and n with V_i.

Figure 20.- Concluded.

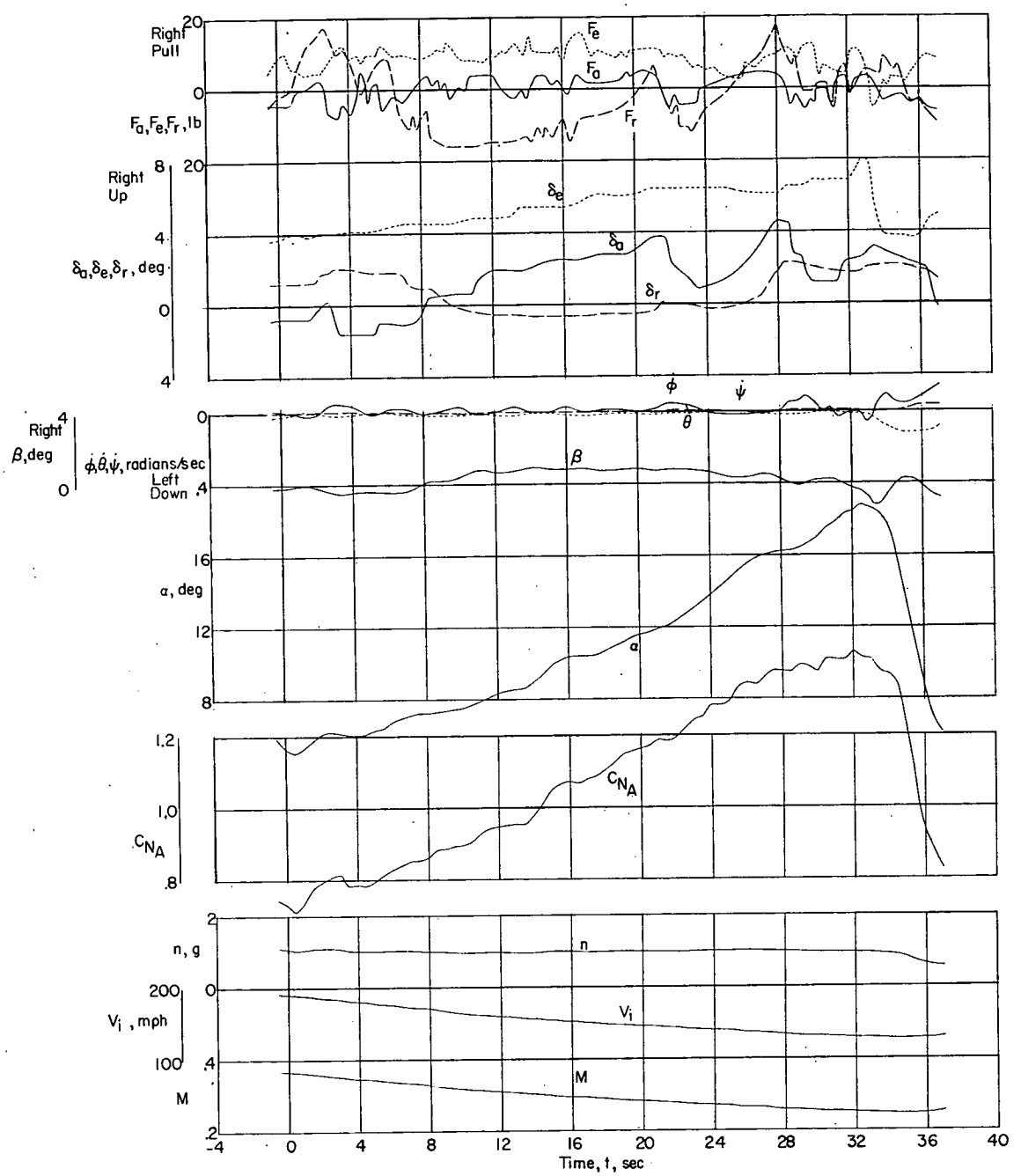

(a) Time history.

Figure 21.- Flight characteristics of the D-558-II research airplane during an unaccelerated stall. Inboard fences on; slats fully extended; flaps extended; landing gear extended; $i_t = 1.6^\circ$; center of gravity at $0.252\bar{c}$; $h_p \approx 20{,}200$ feet.

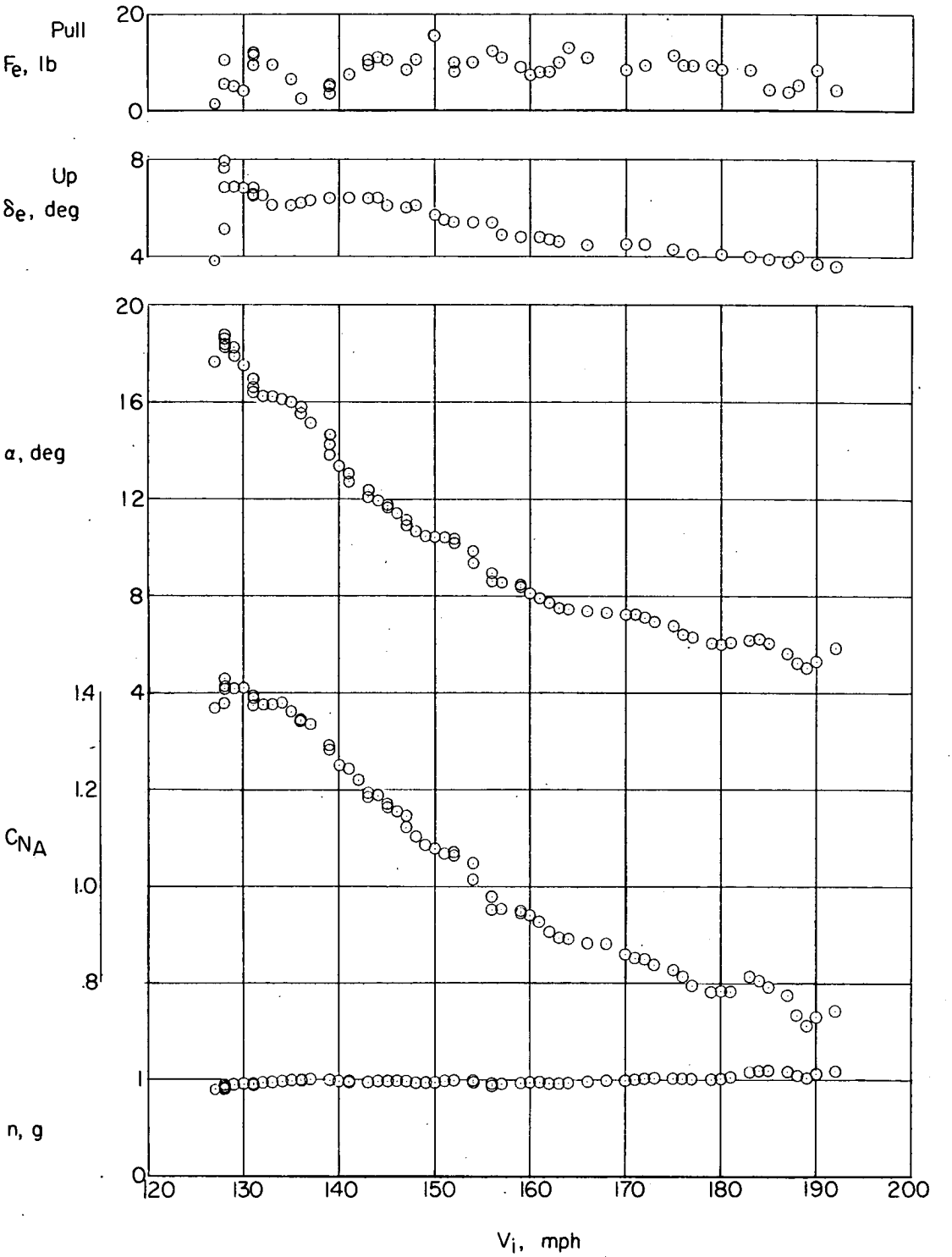

(b) Variation of F_e, δ_e, α, C_{N_A}, and n with V_i.

Figure 21.- Concluded.

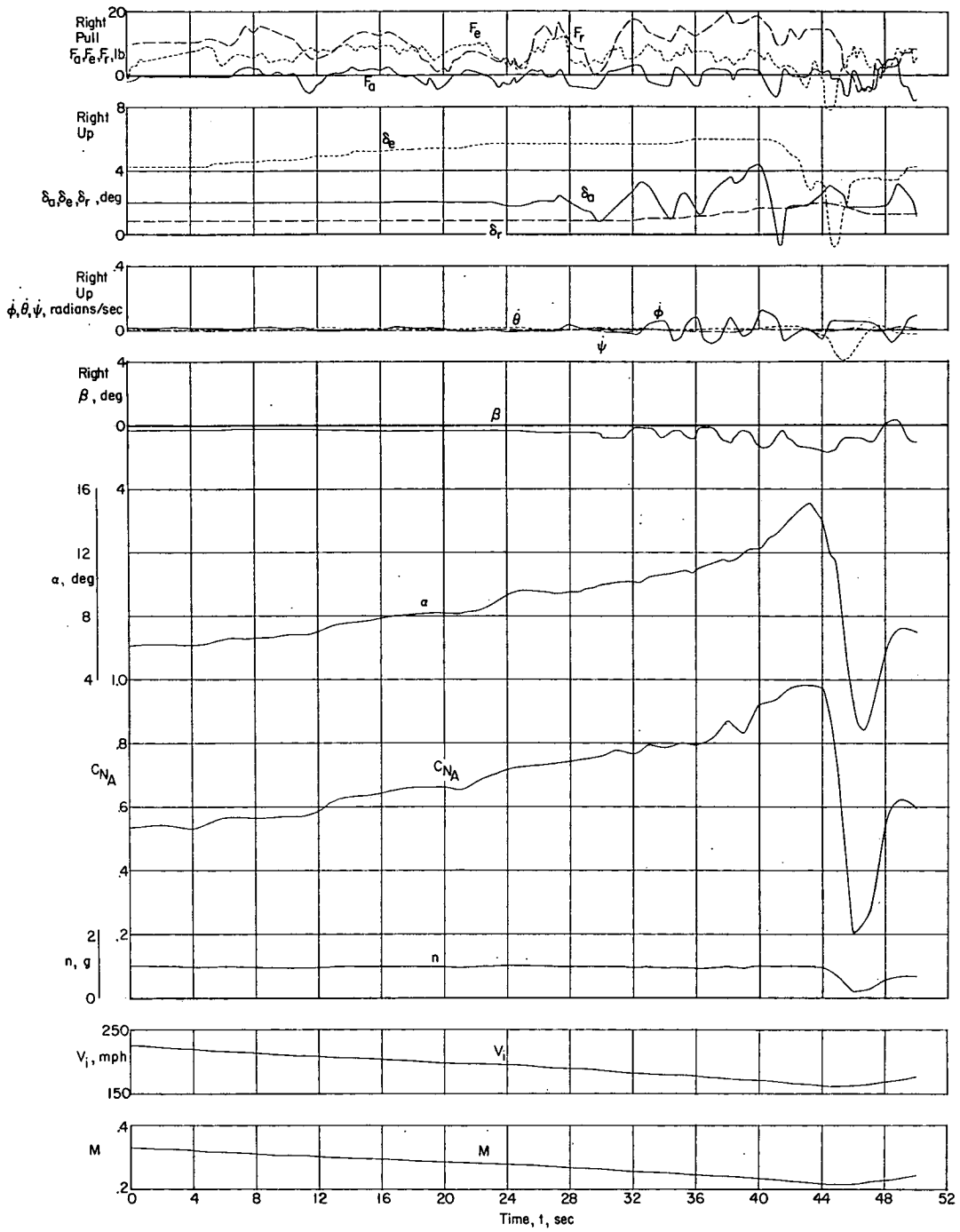

(a) Time history.

Figure 22.- Flight characteristics of the D-558-II research airplane during an unaccelerated stall. No fences on; flaps retracted; landing gear retracted; chord-extensions on; $i_t = 1.6^\circ$; center of gravity at $0.228\bar{c}$; $h_p \approx 20{,}400$ feet.

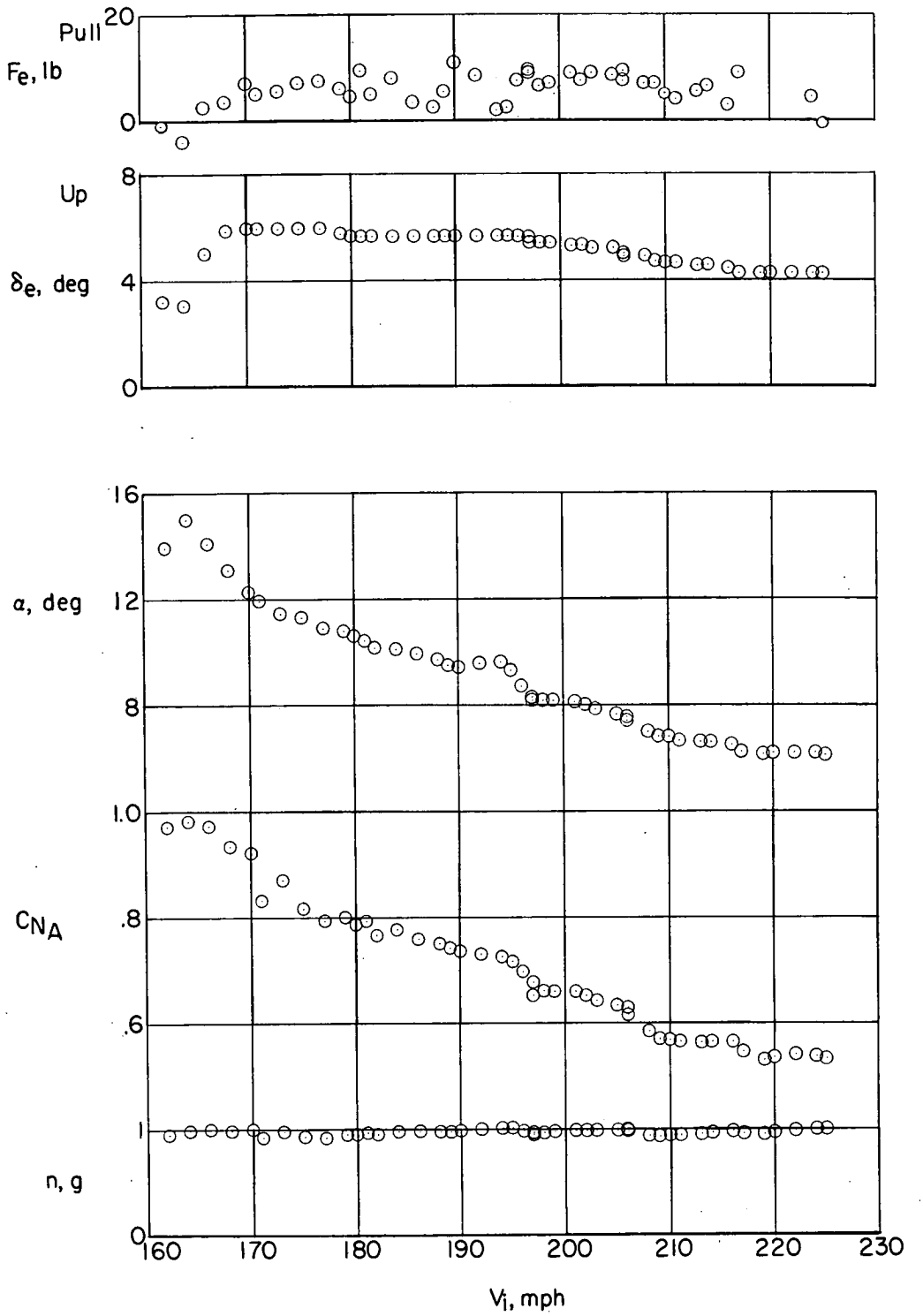

(b) Variation of F_e, δ_e, α, C_{N_A}, and n with V_i.

Figure 22.- Concluded.

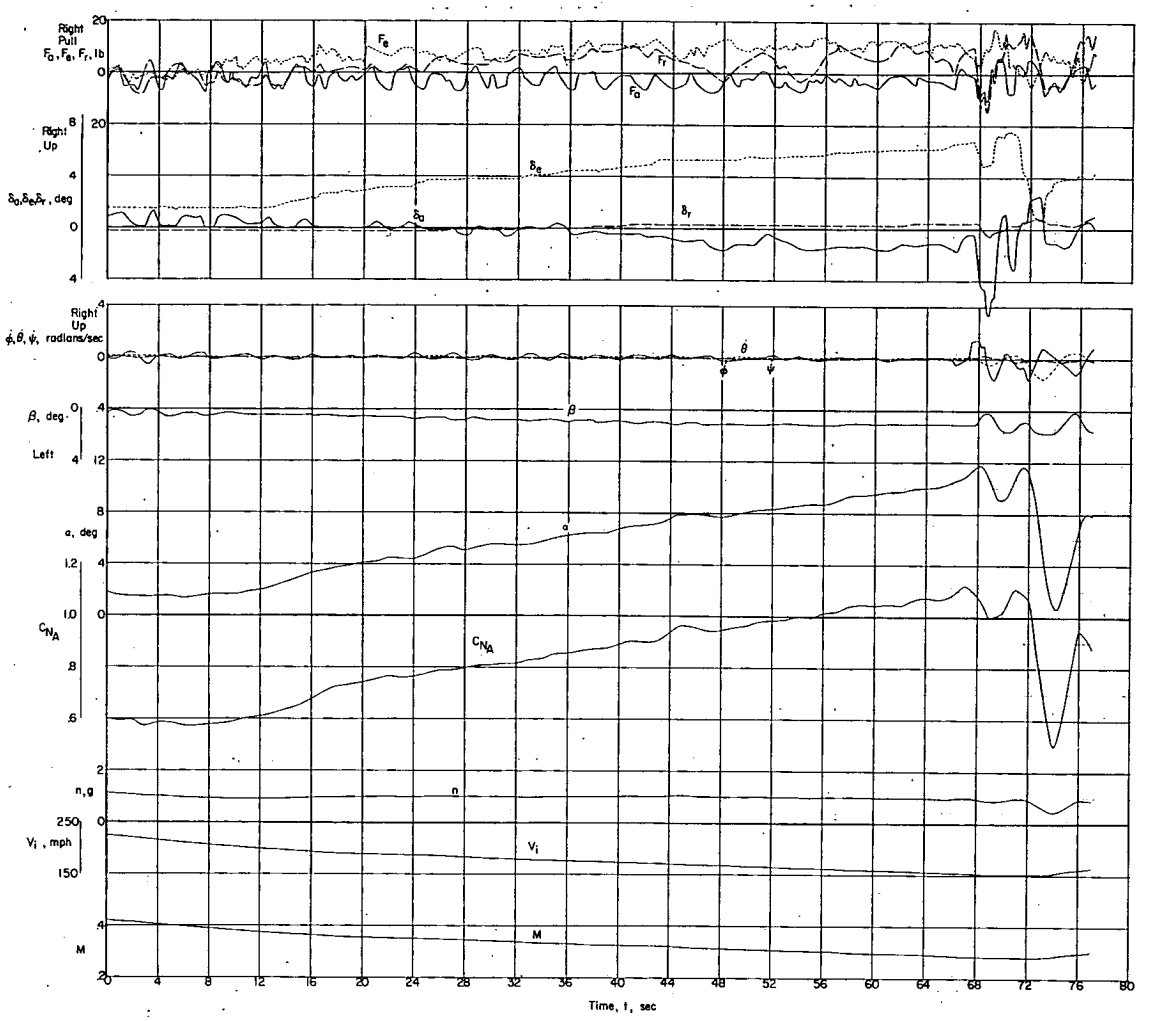

(a) Time history.

Figure 23.- Flight characteristics of the D-558-II research airplane during an unaccelerated stall. No fences on; flaps extended; landing gear extended; chord-extensions on; $i_t = 1.6^\circ$; center of gravity at $0.224\bar{c}$; $h_p \approx 18{,}700$ feet.

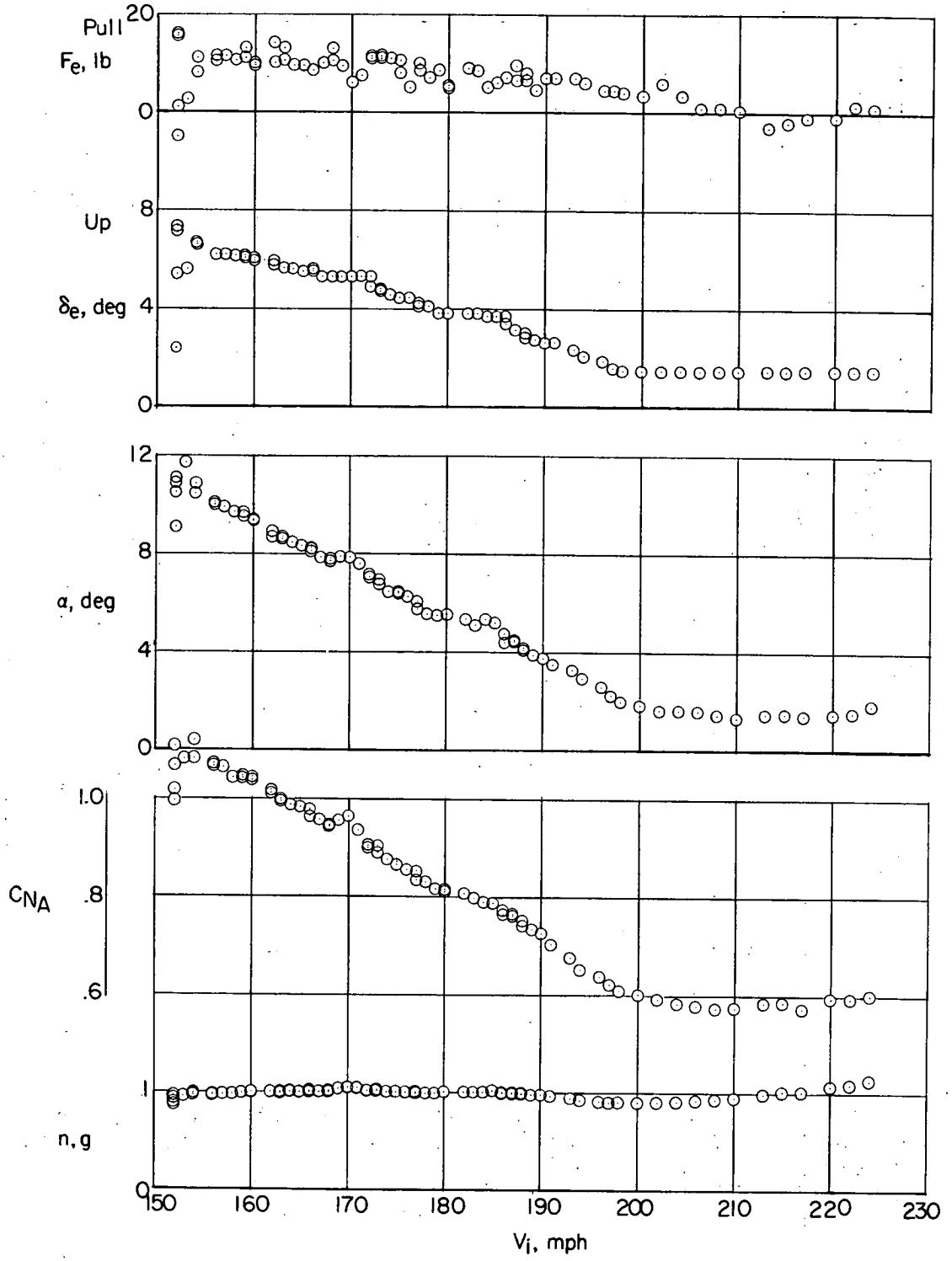

(b) Variation of F_e, δ_e, α, C_{N_A}, and n with V_i.

Figure 23.- Concluded.

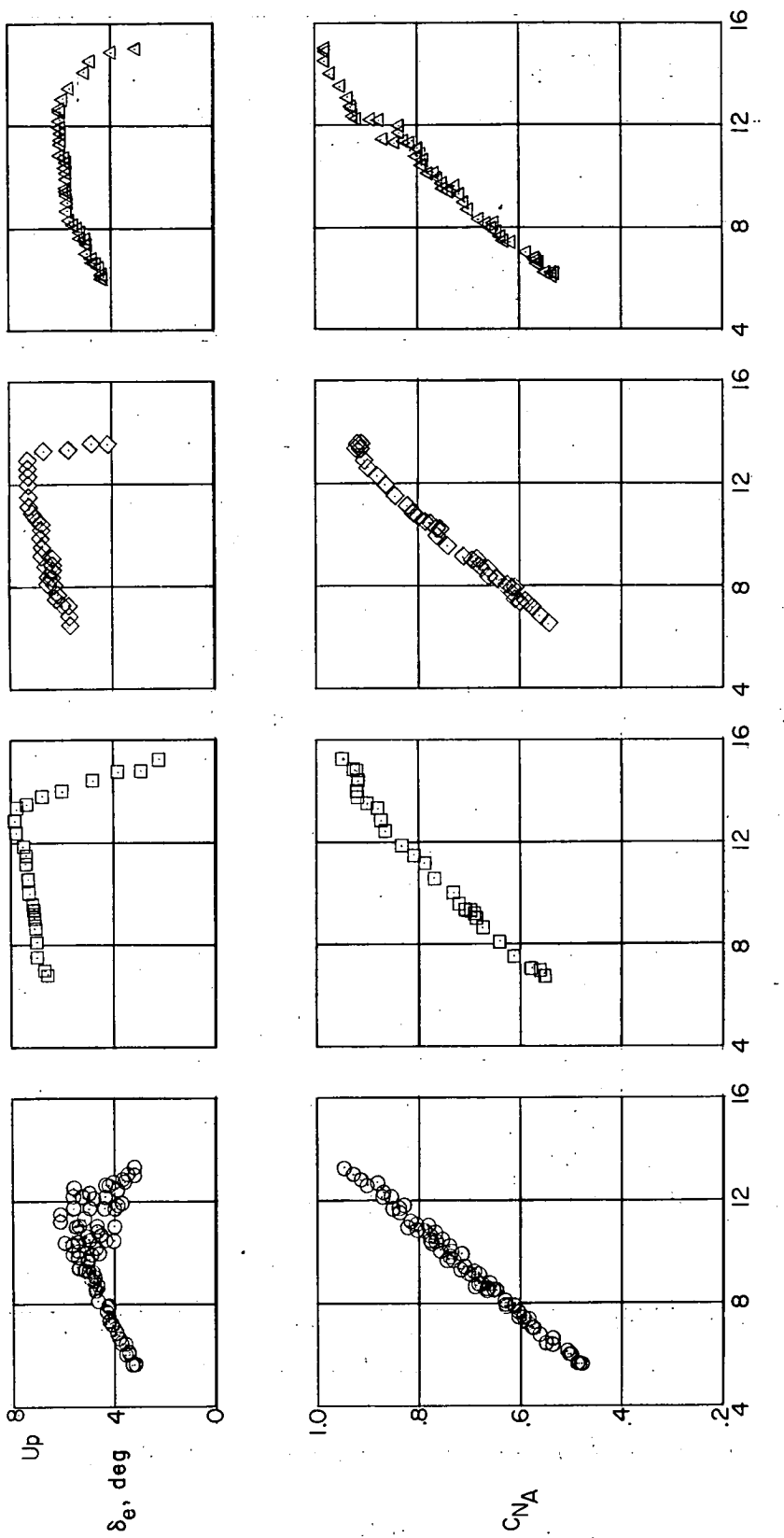

Figure 24.- Comparison of apparent stability and lift characteristics of the D-558-II research airplane with various wing modifications. Wing slats retracted; flaps and landing gear retracted.

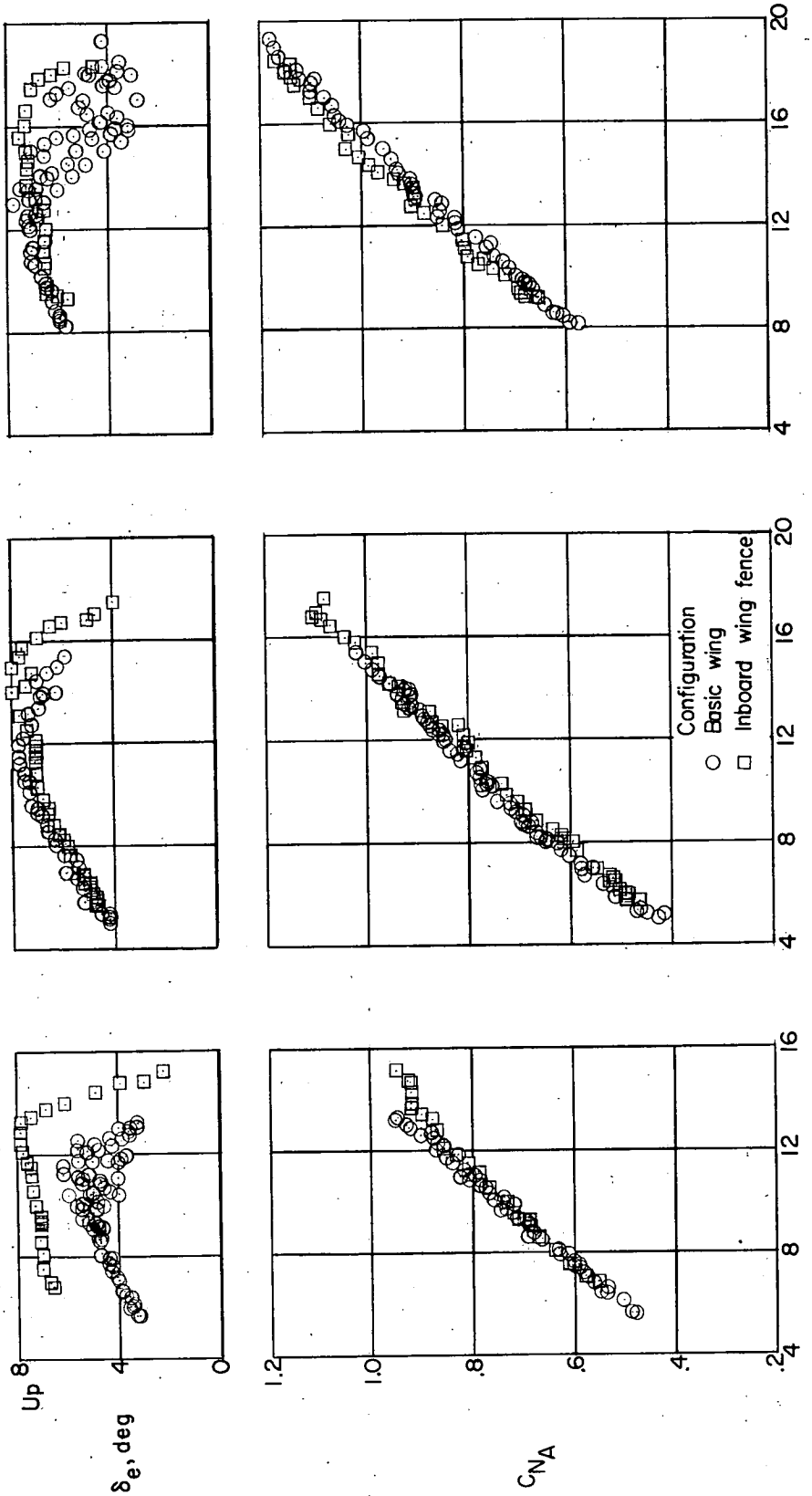

(a) Slats retracted. (b) Slats unlocked. (c) Slats extended.

Figure 25.- Comparison of apparent stability and lift characteristics of the D-558-II research airplane with various wing modifications. Flaps and landing gear retracted.

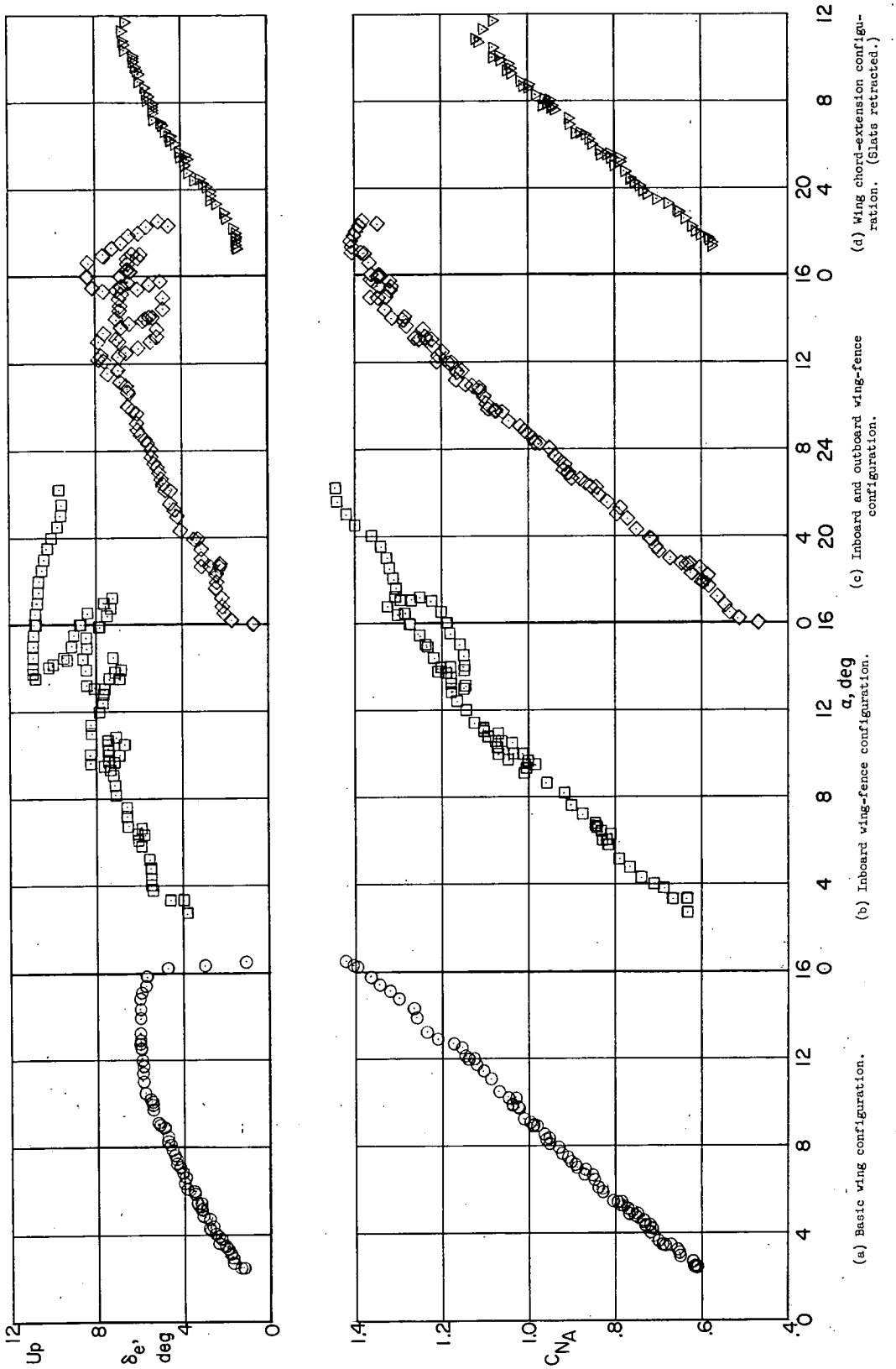

Figure 26.- Comparison of apparent stability and lift characteristics of the D-558-II research airplane with various wing modifications. Wing slats unlocked; flaps and landing gear extended.

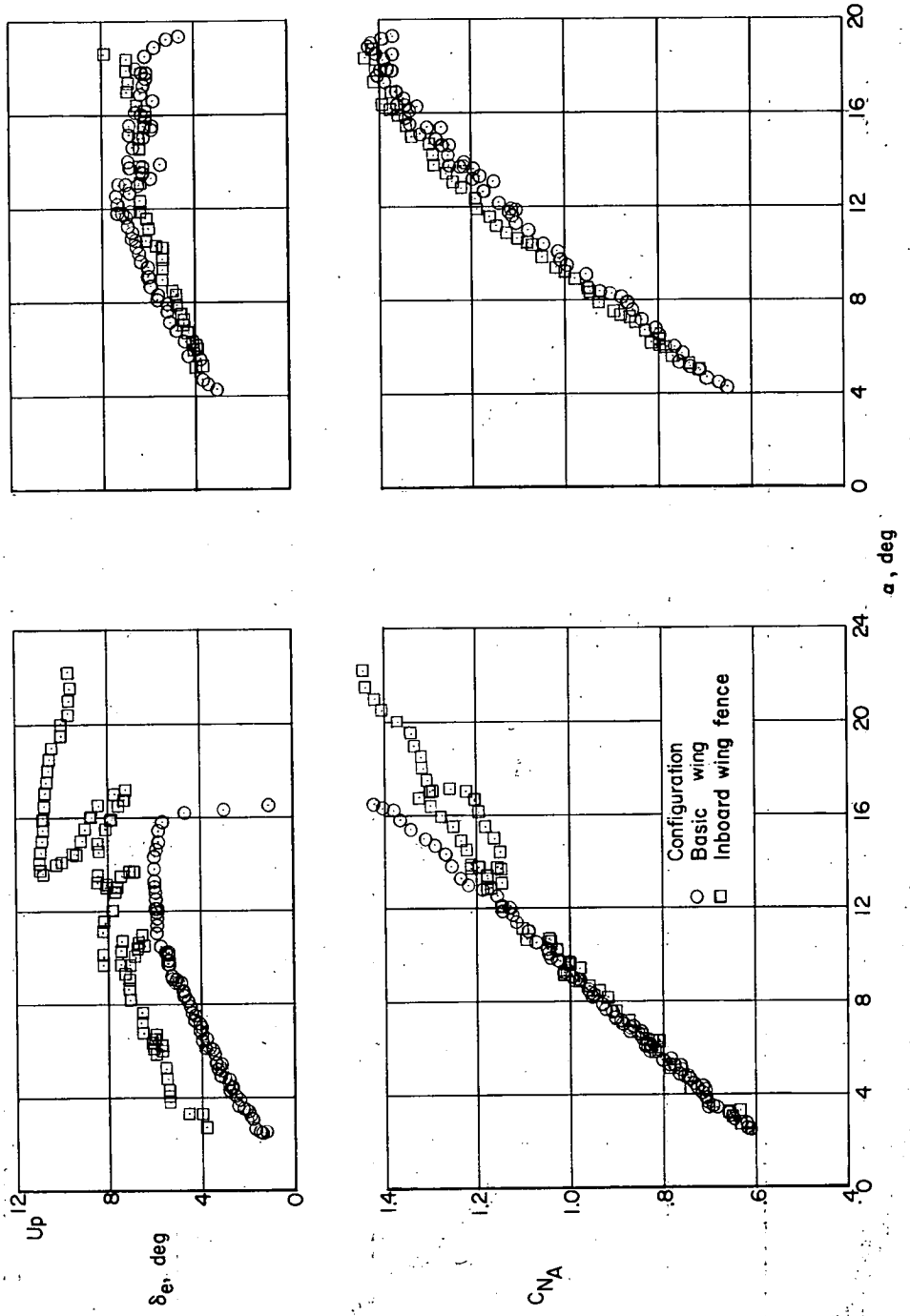

(a) Slats unlocked. (b) Slats extended.

Figure 27.- Comparison of apparent stability and lift characteristics of the D-558-II research airplane with various wing modifications. Flaps and landing gear extended.

NACA - Langley Field, Va.